High Pressure Phases of Group IV and III-V Semiconductors

Department of Physics and Astronomy, The University of Edinburgh
Edinburgh, EH9 3JZ, Scotland, United Kingdom

CONTENTS

The currently known structures and properties of group IV elements and III-V compounds at high pressure are reviewed.
Structural properties of various phases, as determined by experimental techniques, predominantly X-ray crystallography using diamond anvil cells are covered first. The relative equilibrium stability of these phases, as determined by theoretical methods is also discussed. Metastable phases and the processing techniques by which they can be made are examined, introducing the importance of phase transition kinetics in determining what is actually seen.
Elastic and vibrational properties are then considered, looking at how elastic constants and phonon frequencies are affected by increasing pressure and how this can help us to understand the phase diagram and transition kinetics. Finally, using these ideas, it is shown how one can formulate equilibrium pressure-temperature equations of state for these materials.
Throughout, the review draws on both experimental and theoretical work, and emphasises features which seem to be generic to these tetrahedral semiconductors and their high pressure phases.

I. INTRODUCTION

A. Pressure

Notwithstanding the intense scientific and technological interest in the nature of materials in planetary cores or subject to nuclear explosions, the behaviour of materials extreme conditions has long been a subject of speculation and extrapolation. Until recently the methods available to physicists have precluded direct study and left scientists in more applied fields in frustrating or frightening uncertainty.

Over the last few years, study of materials under high pressure has become an extremely important subject displaying explosive growth. This is primarily due to both theoretical and experimental developments which have at last facilitated such work.

Experimentally, high-pressure studies are often confronted with practical difficulties which substantially complicate measurements. These arise from the fact that high pressure can often be generated only in very small sample volumes with a container which may affect the signal. The major development towards overcoming these difficulties is the diamond anvil cell (DAC), in which the hardness of diamond is used to apply the pressure, and its transparency to facilitate the signal (Jayaraman, 1983 Mao and Bell 1979). With DACs it is possible to perform a vast range of experimental measurements at high pressure. These include x-ray and neutron diffraction, extended x-ray absorption fine structure (EXAFS) vibrational spectroscopy and optical measurements. Only the relevant details of these experimental techniques are discussed here as they have been reviewed extensively (Nelmes et al , 1998; Itie et al, 1993; Ohsumi et al, 1986; Weinstein and Zallen, 1984; Spain, 1987, Prins et al, 1989, Jayaraman, 1983)

In addition to these experimental advances, reliable computational methods for electronic structure and total energy calculation have made a substantial impact on high pressure physics. Algorithmic developments (Yin and Cohen, 1982; Car and Parrinello, 1985) and rapid increases in computer power make reliable theoretical calculations of structural, electronic and vibrational properties of materials almost routine. These calculations provide important complementary data to the experimental work, determining which observed structures are thermodynamically stable, indicating the assignment of electronic and vibrational excitation modes, and predicting stability of as yet undiscovered structures.

Implementation of new computational algorithms has been particularly valuable in dealing with complex structures containing several free internal parameters. This is because they allow for simultaneous relaxation of the electronic and ionic positional degrees of freedom. The "relaxation" of the ionic positions proceeds by moving the ions under the influence of Hellmann-Feynman forces until the calculated forces are below some threshold value. The majority of these calculations employ the density functional theory (Hohenberg and Kohn, 1964 Kohn and Sham, 1965) and use local approximations for the exchange and correlation contributions to the total energy (see e.g. Perdew and Zunger 1981, Perdew and Wang 1991, based on work by Ceperley and Alder, 1980 or Ernzerhof et al 1996).

Density functional theory itself and its computational implementation have also been the subject of several detailed reviews (Christensen, 1998; Payne *et al*, 1992;

Jones and Gunnarsson, 1989; Devreese and Van Camp, 1984; Hemley and Ashcroft, 1998).

Pressure is a particularly attractive thermodynamic variable to exploit in such first principles calculations because it affords the possibility of studying the variation in the properties of solids as interatomic distances are changed in a systematic way. In this respect, the effects of pressure are more easily incorporated into first-principles simulations than those of temperature, which requires sampling of many configurations.

B. Semiconductors

On account of the explosion of information technology and computing, the late twentieth century has come to be regarded as the semiconductor age. The technological impact of these materials will be extremely familiar to the reader, so we consider here the atomic level structure of these materials.

Structurally, most semiconductors consist of a network of covalent bonds leading to an open crystal structure which, like water, becomes denser on melting. They typically exhibit a series of high pressure phase transitions to progressively denser structures and have thus become a paradigm for high pressure studies. In the specific case discussed here, the group IV elements and III-V compounds exhibit tetrahedral coordination under ambient conditions, typically in the diamond structure (zincblende or wurtzite in compounds). The application of high-pressure probes the physics of interatomic bonding extremely thoroughly: it gives rise to more dramatic changes in the physical properties of semiconductors than can be attained through temperature variation alone, including bandgap closure and metallisation. Combined with the propensity of covalent materials to form long-lived metastable structures, it is not surprising that the high-pressure properties of semiconductors are at the forefront of crystallographic study.

Chemically, the diamond structure can be regarded as a network of covalent bonds, with secondary ionic bonding giving rise to zincblende or wurtzite ordering in the III-V compounds. Electronically these semiconductors are semiconducting! Application of pressure tends to broaden the electron bands and hence reduce the bandgap: in most cases the first pressure-induced phase transition corresponds to the closing of the bandgap and metallization of the sample: an example of this occurs in tin where the familiar metallic β-tin can be transformed into a grey crumbly powder at low temperature. This is α-tin which has the diamond structure.[1]

A final important effect of pressure in semiconductors, outwith the scope of this review, is its ability to affect the local structure around a crystal defect, and consequently to move the electronic levels associated with such defects. This requires relatively low pressures compared to those involved in phase transitions, and makes pressure a valuable tool for investigating the nature of the defects which give rise to donor or acceptor levels.

II. BASICS

A. Thermodynamics

The underlying quantity which determines phase stability in high pressure systems is the Gibbs free energy

$$G = U + PV - TS \tag{1}$$

Where U is the total internal energy, P the pressure, T the temperature, S the entropy, and V the volume. In all practical applications we are interested in a constant pressure ensemble in which pressure and temperature are applied externally and energy, volume and entropy are free to adjust to these inputs so as to minimise G.

The equation shows the underlying competition that governs the stable structure: as pressure increases structures with lower specific volume become favoured, even if they have higher internal energy. It also shows why temperature is less effective in producing solid-solid phase transitions: it is associated with the entropy, the primary contribution to which (configurational uncertainty in the atomic positions) is the same[2] in all crystals (but significant in liquids and gasses).

For hydrostatic pressure there is a further constraint which the structure must satisfy, namely that the stress tensor σ_{ij} must have the form:

$$\sigma_{ij} = \frac{d^2U}{d\epsilon_i d\epsilon_j} = \begin{pmatrix} P & 0 & 0 \\ 0 & P & 0 \\ 0 & 0 & P \end{pmatrix} \tag{2}$$

where ϵ_i is the strain in the i direction and P is the external pressure.

In comparing theoretical candidate structures, only those satisfying the above constraint should be considered for the hydrostatic phase diagram. It is possible,

[1] a number of historical anecdotes accompany this transition, sometimes known as 'tin pest'. Apparently the officers in Napoleon's army had tin buttons on their greatcoats while besieging Moscow, while Scott took food in tins to the Antarctic. In both cases the phase transition, induced by cold weather, contributed to the ultimate failure of the venture.

[2] a smaller entropy difference does arise due to the vibrational entropy of phonons

however, that other phases could be observed under non-hydrostatic conditions such as in shock waves or the strain field associated with a crack. (e.g. Ackland 1998).

A corollary of the NPT thermodynamic[3] ensemble is that two phases cannot coexist over a range of externally applied pressures.

B. Kinetics and Metastability

In a real material, there may be kinetic barriers that prevent or delay transformation to the equilibrium structure. This leads to hysteresis in the transformation - but if there is a third (metastable) structure with an easier transformation path the material may transform to that instead. Metastable structures can be very long lived, making experimental determination of the true equilibrium phase extremely difficult.

Metastable structures are particularly prevalent in covalently bonded materials: diamond structure carbon, BC8 silicon, etc. reflecting the slow self diffusion in materials where bond making and breaking is involved.

A related phenomenon is the appearance of 'intermediary' phases. These typically appear when there is more than one type of atom or bonding: for example under pressure there may be a large free energy gain when a covalent bonding network collapses from fourfold to sixfold coordination (e.g. in a diamond - β-tin) transition giving a metallic sixfold structure. A smaller free energy gain may then be obtained by ordering the atomic species within the sixfold coordination, to optimise the ionic contribution to the binding. If the second process is slow on the timescale of the experiment, the defective sixfold structure may appear to be a stable phase. A telltale sign of an intermediary phase is a broadened diffraction pattern out of which the equilibrium phase ripens with a sharp pattern, or a thermodynamic anomaly such as the decrease in density with increase in pressure observed in InSb (see below).

C. Crystallography

X-ray crystallography is the standard tool for determining structures. In most applications, single crystal work is the method of choice, however for high pressure semiconductor applications it is usually impractical because the single crystal is shattered in the phase transition. Thus powder diffraction is generally used In principle, crystallography should reveal the exact symmetry of the system, but in practice weak diffraction peaks corresponding to small symmetry-breaking distortions may be unobservable. Resolution of such features has improved enormously in recent years, largely through the shift from energy dispersive studies (Ruoff, 1988, Weir et al, 1989, Vohra et al, 1986, Duclos et al, 1990) to angle dispersed with area detectors to capture data (Cernik et al, 1992). These give accurate peak intensities after integration around the Debye-Scherrer rings (Shimomura et al, 1993; Nelmes and McMahon, 1994). Thanks to the improved resolution, the 'experimentally observed' crystal structures have been reported to be increasingly complex.

It is important to note, however, that reported crystallographic results have been subjected to Occam's razor: they are the simplest possible structure consistent with the data. Although some very recent work has begun to draw conclusions from absent peaks, particularly for ordering (e.g McMahon et al, 1994), symmetry-breaking distortions, remaining undetected through their small size or through microdomain formation always remain a possibility. Moreover, the diffraction results give the mean positions of the atoms within the unit cell, averaged over the whole crystal. Most theoretical approaches assume that this corresponds to the minimum energy position of the atoms - strictly this is only the case for a harmonic crystal - the mean atomic position (as determined from diffraction) need not be the mode (minimum energy).

X-ray crystallographic data probe the long-range time-averaged structural ordering of the crystal: in some cases short-ranged static or dynamic ordering, typically of lower symmetry, may occur as a precursor to the onset of long-ranged order. In these cases, other probes such as microscopy, EXAFS, Raman and transmission spectroscopy (see below) may detect the onset of short range order at different conditions of pressure and temperature (Besson et al 1991). This means that one must be careful about defining exactly what is meant when interpreting experimental results as showing a 'phase transition'.

D. Pressure

Although the SI unit of pressure is defined in terms of force per unit area, the experimental measurement of pressure is usually determined by looking at the frequency of a fluorescence line in ruby (Piermarini et al, 1975). This is related back to SI via the equation of state for a standard material (rocksalt) which equation of state is itself derived from an early electronic structure calculation (Decker, 1971). At higher pressures the ruby scale is calibrated from shock wave data (Bell et al, 1986) There has been some conflict between X-ray and optical

[3] N refers to the number of atoms, presumed constant

calibration (Vohra et al 1988) and even a suggestion that the ruby itself might undergo a phase transition, making pressure measurement dependent on the history of the ruby (Thomson, 1996)

In calculations, the pressure is precisely defined within the approximations of the methods (see section IIID). However, within DFT the local density approximation (Perdew and Zunger, 1981). invariably gives too small a volume at ambient pressure. There is evidence that this can be viewed as a spurious imposed overpressure which should be subtracted in the comparison with experiment (Akbarzedeh et al 1993). More recent calculations have used various 'generalised gradient approximations' (Perdew et al 1992, 1996) which tend to alleviate this problem.

In sum, both theory and experiment have their own internally consistent pressure scale. Neither is uncontroversially mapped to SI and so one should be careful when comparing experimental and calculated 'pressures'.

E. Diamond Anvil Cell

The diamond anvil cell is the single most useful experimental tool in high pressure experimentation (for a review, see Jayaraman 1983). It has been extensively reviewed, and so here we discuss features of direct relevance to understanding properties of high-pressure semiconductors. (Mao and Bell, 1979; Dunstan and Spain, 1989; Spain and Dunstan 1989). Firstly, the geometry consists of two opposed diamonds that are brought together. Thus the pressure is applied by *uniaxially* reducing the volume, with the sample held in place by means of a gasket. Ordinarily, some fluid such as a methanol-ethanol mixture, argon, helium or hydrogen can be used used as a pressure transmitting medium. Typically, the sample volume exceeds that of the fluid medium, and at high pressures the 'fluid' solidifies. Consequently, it may be appropriate to think of the sample as a composite solid, in which the applied stress is supported unequally and anisotropically by the crystallites in the sample. The consequence of this is the observed coexistence of phases across a range of pressures (as measured by the ruby fluorescence) in direct violation of hydrostatic thermodynamics, and a steady variation in measured pressure with volume as the sample is compressed.

A secondary effect of the DAC geometry is that it promotes preferred orientation - prolate or oblate crystallites will tend to orientate themselves with their long axes perpendicular to the cell axis. This leads to imperfect powder sampling which alters the observed intensities of various Bragg peaks: the very data that is required for accurate determination of atomic positions. The *existence* of peak is not affected[4] , so a sample which suffers from preferred orientation will yield reliable crystal symmetry, but unreliable internal coordinates. Within the context of powder crystallography significant efforts have been made recently to overcome preferred orientation effects by rotating the entire DAC (Belmonte, 1997).

F. Pressure and temperature phase diagram

Pressure-temperature phase diagrams are the clearest way to present structural data. However, the reliability of the equilibrium data, both experimental and theoretical, is currently such that they must be taken with some caveats. For example the vast majority of DAC experiments are conducted by increasing pressure at a rates as fast as GPa/minute. This means that any hysteresis or kinetic sluggishness in the transition will cause the reported transition pressure to be too high, perhaps by a different amount for different types of experiment (Besson et al, 1991)[5]. Phase coexistence in DACs is invariably reported, confusing the definition of an exact transition pressure further.

In situ work at simultaneously high temperatures and pressures is now becoming possible, and the computational reliability of entropy calculation lags far behind that of total energies. Consequently the structures existing stably at high temperature are less reliably determined theoretically.

The systems here are characterised by significant hysteresis or irreversibility in their phase transitions. Consequently, phase diagrams presented in this paper are schematic rather than definitive: in general current data is not sufficient to determine accurately the position and slopes of the phase boundaries: even the sign of their slopes in uncertain in many cases.

G. Phonons

Phonons in high-pressure semiconductors can be measured by inelastic neutron scattering, infrared spectroscopy or light (Raman) scattering - the latter two probe only zone centre modes, but have the advantage

[4] In extreme cases, it may become so weak as to be undetectable

[5] And a general trend for more recent papers to report lower pressures, for example the first phase transition in silicon was reported at 20GPa by Minomura and Drickamer in 1962, 16GPa by Jamieson (1963), stabilising at 11.3GPa (Hu et al, 1986, McMahon et al, 1994).

that relatively small samples are required. The zone centre limitation can be surmounted by studying two photon scattering, which enables the Brillouin zone boundary modes to be studied (see section VE).

Phonon frequencies can also be calculated by a number of methods: in the 'frozen phonon' method a calculation is performed on a unit cell in which the atoms have been displaced according to their known eigenvector. More generally, the full spectrum can be calculated either by lattice dynamics Born and Huang (1956) using force constants calculated from finite displacements (Ackland et al 1997), or using DFT linear response theory Giannozzi (1991).

An interesting difference between the methods is that the experimental probes all measure the *correlation function*: i.e. how frequently the mode performs a full oscillation. By contrast the theoretical techniques probe the *curvature of the potential surface*, and use this to evaluate frequencies assuming the vibrations to be harmonic. In harmonic crystals these are equivalent, but anharmonic effects manifest themselves differently.

H. Mechanical Instability

When structures are considered by calculation at 0K, it is possible that they are unstable with respect to symmetry-breaking strain (elastic instability), atomic motion (phonon instability) or some combination. It is also possible that such instabilities develop with increasing pressure.

High pressure introduces some additional complexities into calculating such distortions. Assuming hydrostatic pressure, equations 1 and 2 hold and we must consider minimising the free energy (or enthalpy at 0K). This introduces modifications to the conventional Born elastic stability criteria as discussed in section VIA. It also means that where the transition involves a softening phonon and a coupling to strain, that phonon frequency will not go to zero, since the vibrational mode frequency is determined by $\frac{d^2U}{d\nu_i^2}$ not $\frac{d^2H}{d\nu_i^2}$ (where ν_i represents the atomic displacements associated with the phonon, and H is the enthalpy). Only in a truly second order transition ($\Delta V = 0$) would the phonon frequency drop to zero at the transition: in the III-V semiconductors a possible candidate is the rocksalt-$Cmcm$ structure in InP.

III. THEORY

A. Simple mechanical models

The lowest level of theoretical analysis possible for high pressure structures is to consider packing of spherical atoms. This explains the trend from open structures to more close packed ones with increasing pressure, and the associated increase in coordination. Atomic ordering can also begin to be understood at this level, with the simple hypothesis that unlike near neighbours are preferred over like ones. However, packing ideas shed no light on why open structures exist in the first place.

To go further, we must consider electronic structure. For tetrahedral phases, the simple picture is to consider the atoms joined by covalent bonds, one for every pair of electrons (here on average four per atom). This can be modelled by representing the bonds by rigid rods which repel one another. This simple model gives a phase diagram in which diamond $\rightarrow$ $Imma$ $\rightarrow$ simple hexagonal $\rightarrow$ fcc, with β-tin existing as a high temperature phase(Ackland, 1994).

Combining a model of four repelling rigid rods with the principle of unlike nearest neighbours produces a generic phase diagram containing most of the lower pressure observed structures for the less ionic compounds.

B. Semiempirical potentials

There is a huge literature of semiempirical potentials, particularly for silicon, based on a physically reasonably functional form parameterised to fit experimental data. It is not unusual for high pressure phases to be included in the fitting dataset, but there have been very few applications of such potentials to high pressure transitions. The reason for this seems to be that they do not work well - a single functional form being unable to describe the tetrahedral covalent bonding of the ambient phases and the metallic bonding of the high pressure phases (see the comparative study by Balamane et al 1992). One noteworthy contribution (Piltz et al, 1995, using a potential by Ackland, 1991) came in solving the R8 phase of silicon by a small distortion from BC8: a simple situation where the covalent nature of the bonding is similar in each phase. Another use is to establish the effects of finite size or short simulation time on simulations: the simulations relate to an artificial material, "empirical potentialium" rather than silicon, but give an accurate picture of how quantities which *can* be evaluated for real materials (e.g. static transition barriers or elastic constants, energy differences between phases, harmonic phonons) are related to statistical quantities which cannot (phase transformation rates, finite temperature elasticity etc.)

Other uses are to overcome finite size effects in molecular dynamics calculation when the relevant static behaviour is well characterised, even if not quantitatively accurate for the real material (e.g. Mizushima et al, 1994).

C. Nearly free electron theory

It is perhaps surprising that the nearly free electron theory is applicable to high pressure semiconductors: however even the band structure of diamond silicon has near parabolic bands with distortions and the Brillouin Zone boundaries. Thus the nearly free electron picture makes a good conceptual starting point for discussing band structure effects.

In the nearly free electron picture electrons interact with the lattice, lowering the energy of a structure only when two conditions are met: they have energies near to the Fermi Surface and have a k-vector close to a lattice vector. The strength of interaction between electron and lattice arises from scattering: and hence the Bragg peaks in the X-ray diffraction picture define the k-vectors where the perturbation is strongest. This leads to a simple rule of thumb: structures with diffraction peaks close to the Fermi vector are favoured. An alternative formulation, (Jones 1962) involves forming a near-spherical second Brillouin Zone (for tetravalent materials).

The major triumph of the nearly free electron picture is in describing the c/a ratio β-tin structure. In most materials it is about 0.55 and relatively insensitive to pressure, giving four nearest and two second nearest neighbours, significantly larger than the $\sqrt{4/15} = 0.516$ which would equalise these bondlengths. This seems inexplicable when considered in direct space, but viewed in reciprocal space the value of 0.55 makes the strong (220) and (211) diffraction peaks almost degenerate at k_F. The $Imma$ ($Imm2$ in compounds) distortion serves to bring these peaks even closer together, while the $Cmcm$ structure has a similar set of degenerate peaks at k_F.

One might even go as far as to say that the nearly free electron theory explains why the III-V semiconductor structures have proved so difficult to resolve experimentally - the energetics favour those structures with similar positions of the strongest diffraction peaks!

The Brillouin zone touching argument is based on geometry, thus a further prediction, reasonably well observed in practice, is that the c/a and b/a ratios of stable structures should be independent of pressure.

Impressive as some of these results are, it should be noted that the nearly free electron theory concentrates only on the effects due to a few electrons near the Fermi surface[6]. As a perturbative theory, it has been successful in explaining details of particular structures, but not in describing the relations between different structures.

In recent years, nearly free electron theory has been superceded by more accurate total energy calculations, which incorporate all the effects arising from the electronic structure.

D. Total Energies from Electronic Structure Calculations

Early work demonstrated the power of the total energy method (Froyen and Cohen, 1982, 1983; Yin and Cohen 1982), and the results of the *ab initio* computer calculations reported here are extremely precise. Their accuracy, however, depends on the underlying theory. A typical density functional calculation is subject to the accuracy of the functional used,[7] and the reliability of the input structure. In general, density functional calculation distinguish accurately the relative stability of phases, but can only be applied to known structures. The possibility always exists that the stable crystal structure may have been overlooked by the simulators.

Other sources of error lie in the use of pseudopotentials or finite basis sets for describing the electronic wavefunctions in different structures: since pressure-induced transitions often involve significant changes in the electronic structure, care must be taken to ensure that the methods used are equally accurate in both structures. A final issue is the k-point sampling of the Brillouin zone: This basically determines how many of the 10^{23} electronic wavefunctions are actually calculated to obtain a representative sample from the bulk material, and the total energy does not converge monotonically with increasing k-point sampling. In metals the total energy is particularly sensitive to k-point sampling. To compare similar structures it is sometimes possible to achieve cancellation of errors by using identical k-point sampling (Kelsey and Ackland, 2000). As we saw in the section IIIC, the electronic states near to particular points on the Brillouin zone boundary may be crucial, so more careful sampling may be important in those regions.

Another important aspect of total energy calculation is that the quantity required to determine phase stability is the free energy difference between the two phases. Most ab initio methods make quite significant errors in calculating the total energy, but many of these cancel if they occur in regions near to the atomic nucleus where the electron density is identical in different structures. Differences in free energy arise from different bonding, which in turn comes from the behaviour of the electrons between the atomic cores. This concept of concentrating on the regions important for the problem at hand underlies the pseudopotential concept and helps to explain its success.

---

[6]The k-degeneracy may also contribute to stability through producing extrema in the Madelung energy

[7]This is typically limited by the description of exchange and correlation effects. The most accurate method currently in use for solids, Quantum Monte Carlo, has yet to be applied to the high pressure phases in silicon

There have been a huge number of studies of III-V semiconductors using DFT techniques: where 'total energy calculations' or 'computational studies' are referred to in this review, these are what is intended. Those studies undertaken using the Hartree-Fock method (exact exchange, no correlation) are explicitly labelled.

E. Ab initio Molecular Dynamics and Monte Carlo

To simulate the effects of temperature, one has to sample a representative region of the phase space associated with the crystal structure: i.e. a number of different possible atomic arrangements. To do this, molecular dynamics or Monte Carlo simulations can be performed. Car and Parrinello (1985) introduced an efficient molecular dynamics scheme, which can be supplemented by constant pressure methods (Parrinello and Rahman, 1981; Focher *et al*, 1994; Bernasconi et al, 1995; Warren and Ackland, 1996) to produce representative configurations. Free energy differences can be obtained from these calculations by thermodynamic integration (Frenkel and Ladd, 1984, Alfe et al 2000) or Hamiltonian switching (Bruce et al 1997) between an accurate *ab initio* representation of the energy and a simpler but exactly solvable potential.

An alternate approach is to use the quasiharmonic approximation based on lattice dynamics to evaluate phonon entropiesTaylor et al 1997, Swift, 1999. This method has the advantage that the entire Brilloiun zone can be sampled (unlike molecular dynamics, where finite size effects can be a problem) but th edrawback that anharmonic effects are ignored.

IV. CRYSTAL STRUCTURES

A fuller description (with pictures) of most of the crystal structures described in this review can be found in Nelmes and McMahon, (1998).

A. Tetrahedral Structures: Diamond($Fd3m$), Zincblende ($F\bar{4}3m$), Lonsdaleite($P6_3/mmc$), Wurtzite($P6_3mc$)

These four structures offer the possibility of perfect tetrahedral bonding[8] and contain only even-membered rings of bonded neighbours allowing a unique binary ordering with unlike nearest neighbours.

Cubic diamond/zincblende is the ambient crystal structures of all elements/compounds in this review, with the exceptions of the nitrides which adopt the wurtzite structure, and of graphitic carbon and BN. Hexagonal lonsdaleite and wurtzite appear metastably in other materials, generally after heating a depressurised sample.

All of the III-V semiconductors which adopt the wurtzite structure under ambient conditions, exhibit a smaller than ideal c/a ratio ($c/a < \sqrt{8/3}$) and the stability of wurtzite relative to zincblende has been described in the context of this quantity (Lawaetz,1972). This is supported by total energy calculations for the c/a ratio in metastable wurtzite phases of other III-V compounds which give a positive deviation from ideal. A similar stability relationship is observed between hcp and fcc for close-packed metals. Ueno et al (1992,1994) have investigated this further, finding that in AlN and InN pressure distorts the structure further from ideal, while for GaN no such effect is observed. The distortion in InN is sufficient for Besson et al (1996) and Bellaiche et al (1996) to describe it as an isostructural phase transition.

By analogy with close packed phases, it is possible to construct a sequence of tetrahedrally-coordinated phases with stacking sequences more complex than ABCA (diamond) or ABAB (lonsdaleite), or even randomly stacked[9] . Such defective structures retain the threefold rotation symmetry of the (001) plane, and appear on depressurization in some materials.

In general, phases with these structures are semiconducting or insulating.

B. Distorted Tetrahedral Phases, BC8($Ia\bar{3}$), ST12 ($P4_32_12$), R8 ($R\bar{3}$), SC16 ($Pa\bar{3}$) and cinnabar($P3_121$)

These structures represent ways of packing atoms more efficiently than the open diamond structure, while still retaining covalent-style tetrahedral bonding (Kasper and Richards, 1964). The relationship between BC8, SC16 and R8 is shown in figure1, ST12 and cinnabar involve other covalent network topologies. At high pressure, the enthalpy gain from their smaller atomic volume offsets the cost of distorting the tetrahedra, and they become more stable than diamond/zincblende. However, since they are based on a different topology of covalent bonds direct transformations between different tetrahedrally coordinated phases are not observed.

The one exception to this is the BC8-R8 'phason' transition in silicon which involves breaking and remaking of only one of the 16 bonds per unit cell. Work on these structures was reviewed by Crain et al (1995), and by considering these phases as approximants to icosahedral quasicrystals other possible phason-related phases have been proposed (Dmitrienko, 1999).

---

[8] In wurtzite and lonsdaleite there is a small distortion away from perfect tetrahedra

[9] Many examples of complex or random stacking appear in polymorphs of silicon carbide

Until recently, the binary analogues of these structures had not been reported, the first experimental and theoretical predictions came in 1994 (Hull and Keen in CuCl, Crain et al in GaAs).

Although it has the same spacegroup as the prototype HgS, the cinnabar structure which appears metastably in III-V compounds is fourfold rather than twofold coordinated

Materials with these structures tend to be semimetallic.

C. β-tin ($I4_1/amd$), $Imma$ and $Imm2$

The β-tin structure is an intermediate between four- and six-fold coordination. With a c/a ratio of 0.5164 each atom would have six equidistant neighbours, but in Si (0.549) Ge (0.554) and Sn (0.546) there is a significant departure from this 'ideal' structure, which is only slightly reduced with increasing pressure.

The bonding in 'fourfold' β-tin is topologically identical to that in zincblende, and hence a diatomic form of β-tin with $I\bar{4}m2$ symmetry is often postulated, wherein all four neighbours are of opposite atomic species. In practice this is not observed, (Nelmes et al, 1997) perhaps because a diatomic form of 'sixfold' β-tin can be made with more unlike nearest neighbours.

The $Imma$ structure is a distortion of β-tin, corresponding to a soft Γ-phonon displacement of one sublattice along the c-direction from $(0, \frac{1}{2}, \frac{1}{4})$ to $(0, \frac{1}{2}, \Delta)$. The equivalent structure in compounds has $Imm2$ symmetry. The special case $\Delta = \frac{1}{2}$ gives the $Immm$ structure which can also be viewed as a decoration of the simple hexagonal (see next section). The rocksalt structure can also be obtained as a distortion of β-tin (See Figure 2)

β-tin type structures tend to be metallic.

D. Simple Hexagonal ($P6/mmm$) and its decorations

The simple hexagonal structure is observed in Si and Ge at high pressures: it is an eightfold coordinated structure with close packed planes stacked directly atop one another. In the compounds, stacking perpendicular to the close packed layers consists of alternating species, leading to rocksalt-type square layers.

Since a close packed plane consists of equilateral triangles of atoms, it is impossible to form a diatomic equivalent of the simple hexagonal structure with all unlike-nearest neighbours (Kelsey and Ackland, 2000). There are several ways of decorating the layers to ensure that four of the six neighbours are of unlike species (Figure3). Most entail an orthorhombic distortion[10] with chains of like-atom neighbours. The extreme cases (see Figure 3) are straight chains ($Immm$) and chevroned patterns ($Cmcm$ and super-$Cmcm$, depending on the repeat length). A structure based on irregular chains would exhibit $Immm$ symmetry on average.

The $Cmcm$ phase has only recently been identified as a potential structure, but is now ubiquitous: early work often attempted to fit $Cmcm$ diffraction patterns to the similar β-tin or rocksalt structures, while early calculations did not consider the structure at all. Typical internal parameters are given in table II

Simple hexagonal structures tend to be metallic, with low frequency phonon modes sometimes leading to superconductivity.

E. Rocksalt ($Fm3m$)

The classic sixfold-coordinated NaCl structure is observed at high pressure in the more ionic indium and nitrogen compounds (see Figure 4) Its appearance in the phase diagrams of all the II-VI compounds and the absence of its monatomic equivalent (simple cubic) in the elemental phase diagrams is a testimony to its favourability for ionic rather than covalent bonding. Notwithstanding this, III-V compounds adopting the rocksalt structure tend to be metallic.

F. NiAs ($P6_3mc$)

The hexagonal nickel arsenide crystal structure can be thought of as an hcp stacking of anions with cations located in the octahedral interstices: each atom has six unlike nearest neighbours while the cations have additional like-atom neighbours. It is unrelated to other structures observed in the III-V compounds, and has been reported in AlP, AlAs and AlSb. It represents an efficient packing of large anions and small cations, but the high pressure structures are generally metallic.

G. Amorphous and liquid phases

Highly directional *sp* bonding in most of the above structures gives scope for a multiplicity of defects. Indeed, in most reported solid-solid transitions on increasing pressure, there is a significant concentration of amorphous material - especially for the elemental materials or low ionicity compounds. In general, amorphous phases of

[10] see Kelsey and Ackland, 2000 for a theoretical counterexample

group IV or III-V materials are more dense than the fourfold coordinated structures, similar to the liquid phases. This gives relatively unusual phenomena also observed in water: that for certain temperatures the tetrahedral phases can be melted by application of pressure, and that approaching their freezing point liquid semiconductors exhibit negative thermal expansion. It is difficult experimentally to study amorphous structures in the same detail as crystalline structures, the best method is to use structure factors from neutron scattering data, these can be related to structural models by reverse Monte Carlo analysis (McGreevy, 1992), but even this tends to give multiple solutions and there is a need for a good guess at an initial structure. Because amorphous phases are thermodynamically metastable[11], simulation is also bedevilled by the effect of initial conditions. Some progress has been made:Clark et al (1997) have shown by calculation that even for identical initial conditions, the structure of amorphous carbon and amorphous silicon are wildly different. sp^2 bonding in carbon allows for lower density structures, while in silicon under- and overcoordinated atoms are more common.

Amorphous carbon, in particular, is very dependent on manufacture with some atomic configurations (e.g. three-centre bonds) which are absent in bulk (Marks et al 1996). Using model potentials Tang and Yip (1995) have shown that high pressure amorphisation can be related to elastic shear instabilities.

Experimentally, Tsuji *et al* (1995) have synthesised several amorphous tetrahedrally-coordinated semiconductors from quenched high-pressure phases. Besson et al (1993) and Vohra et al (1990) reported pressure-induced amorphisation in GaAs.

V. STRUCTURAL PROPERTIES OF SPECIFIC MATERIALS

A. The generic phase diagram

Although different structures are observed for different materials, it is possible to identify general trends. The zero pressure structures of the group IV and III-V semiconductors exhibit perfect tetrahedral bonding[12]. At elevated pressures further fourfold coordinated structures are found, for which cohesion is still primarily due to covalent bonding[13]. At still higher pressures sixfold and eightfold coordinated structures are found[14]. Ultimately, the pressure is great enough that valence electrons become delocalised and close packed structures are found.

The low self diffusivity in covalently bonded materials means that metastable structures are often formed and can last indefinitely under ambient conditions. The classic naturally-occurring example of this is diamond carbon, but several recipes have been devised to form other long-lived metastable structures.

Figure 4 shows a schematic pressure phase diagram showing the various observed crystal structures and the compounds adopting them. The ordering of the materials does not correspond to any physical property, it is simply chosen so as to place those materials with similar structures adjacent to one another.

It is also interesting to note the correlations between ambient properties and high pressure behaviour. Figure 5 shows the strong correlation between the ambient lattice parameter and the transition pressure to the first high pressure phase. Other correlated quantities are tabulated in tables 3-5

B. Group IV Elements

1. Carbon

Carbon exhibits two unusual features which make it worthy of separate treatment: sp^2 bonding and extremely high energy of the first d-band. There are four observed crystalline forms of carbon: graphite and fullerene crystals represent low pressure forms based on sp^2 bonding which otherwise occurs only in BN. Diamond is a high-pressure form, while Lonsdaleite (hexagonal diamond) is sometimes found in meteorites or shock-wave recovered samples. Obviously, diamond anvil cells are unable to reach pressures above which diamond transforms, so recent experimental work has left the high pressure phase diagram of diamond untouched.

Computationally, it was discovered that 'close-packed' structures are not only energetically unfavoured in carbon, but also have larger equilibrium volumes per atom than the 'open' diamond structures (Fahy and Louis 1987). As a consequence the only high pressure phase

---

[11]Defining the entropy for an amorphous phase remains a problem in thermodynamics: should one integrate over all phase space configurations which one would regard as 'amorphous' or only those accessible to one particular amorphous structure?

[12]strictly, the hexagonal wurtzite and lonsdaleite structures have bond angle which depart very slightly from the tetrahedral ideal

[13]strictly, some of these structures give rise to semimetallic materials which dramatically affects their transport properties

[14]Chelikowsky, 1987 has related the preferred high pressure structure to ionicity (Phillips and van Vechtin (1970) Garcia and Cohen (1993)

transition predicted in early studies was to BC8, at 1100GPa. More recently, ideas for structures have turned to analogues of those observed in other materials, and several structures have been proposed which appear to be more stable than diamond at extremely high pressures. A fruitful source of candidate structures has come from considering the positions of the silicon atoms in various phases of SiO_2, which also forms linked tetrahedral networks (Teter et al, 1998) the oxygens occupy the positions of 'covalent bonds' in the purported carbon structures). Another possibility is the R8 phase (Clark et al 1995), predicted to be more stable than diamond above 910GPa. By analogy with silicon, this would be kinetically hindered from transforming back to cubic diamond, producing instead hexagonal diamond; consistent perhaps with the Lonsdaleite carbon found in samples recovered from high pressure.

Galli et al (1990) demonstrated that under extreme pressure diamond carbon could be melted, Grumbach and Martin (1996) have considered melting of BC8 and simple cubic carbon at high pressure and suggested a phase diagram.

Thus it is likely that an as-yet undiscovered phase of carbon exists at pressures above that where diamond is stable. However, the reported energy differences between the competing predicted structures is small, and formation kinetics may play an important role, so the precise structure remains an open question. Although the predicted pressures are high, they are comparable with those at the centres of large planets were carbon is believed to be prevalent.

2. Silicon

Silicon exhibits a plethora of stable and metastable high pressure structures which have been discovered since Minomura and Drickhamer reported the first in 1962. Ruoff and Li wrote a review of diffraction work in Si in (1995).

Because of its status as the archetypal material for high pressure studies, many groups have worked on silicon and the nomenclature of the various structures has become rather confused. The sequence of thermodynamically stable low temperature phases with increasing pressure appears to be diamond-*Imma*-SH-*Cmca*-hcp-fcc, where the orthorhombic "Si-VI" phase (Olijnyk et al 1984, Duclos et al 1990, Vijaykumar and Sikka, 1990) has only recently had its crystal structure identified (Hanfland et al 1999, Ahuja et al, 1999) with *Cmca* symmetry and a 16 atom unit cell.

The β-tin phase is observed at room temperature and pressures between diamond and *Imma* stability, but calculations and theoretical analysis suggest it will not persist to 0K.

Further complications arise from the irreversibility of these transitions: once silicon has passed through its first phase transition to β-tin the diamond phase cannot be recovered simply by depressurisation. Instead depressurised silicon transforms through two distorted semimetallic tetrahedral phases which total energy calculations show to be metastable: R8 and BC8 (Biswas et al 1987, Clark et al 1994, Crain et al 1994, Pfrommer et al 1997), or surface stabilised (Clark et al 1994). The BC8 phase persists indefinitely at ambient pressure and room temperature, but on heating transforms to what was originally reported as a hexagonal diamond structure, but now seems more likely to have a more complex or random stacking sequence as discussed in section IVA (Besson et al 1987, Nelmes et al 1993).

Total energy calculations in silicon have proved remarkably accurate: Needs and Martin (1984) posited that the reported 'β-tin' phase should be unstable with respect to a soft-mode transition to *Imma*, improved experimental resolution made this structure detectable by McMahon et al. (1994). The soft mode associated with this, and the transition to simple hexagonal, leads to enhanced superconductivity in these phases (Chang and Cohen 1985, Mignot et al 1986). The *Imma* $\rightarrow$ β-tin energy differences are very small: Lewis and Cohen, 1993 predict that *Imma* is stable at all pressures (at 0K) while FP-LMTO [15] calculations by Christiansen (1998) do find a region of β-tin stability. Since the β-tin phase has higher entropy, both of these calculations can be regarded as consistent with the room temperature experimental data.

The diamond$\rightarrow$ β-tin phase transition is kinetically very difficult: a mechanism of continuous deformation in which the diamond structure in uniaxially compressed along (001) is geometrically possible, but total energy calculations showed it to have an extremely high energy barrier. Rapid pressurisation tends to bypass the β-tin phase altogether, as do computer simulations using constant pressure ab initio molecular dynamics (Bernasconi et al 1995). The reverse transition does not occur at all, further indicating the absence of a low energy transformation path.

[15]The full potential linear muffin tin orbital (FP-LMTO) method is based on density functional theory, but incorporates all electrons explicitly rather than using pseudopotentials as do the other calculations reviewed here. It also uses a localised basis set to describe the wavefunctions. FP-LMTO calculations are generally regarded as having similar accuracy to other DFT-based ab initio methods

3. Germanium

Germanium has essentially the same phase diagram as silicon, with the diamond phase transforming to β-tin (Baublitz and Ruoff, 1982) and then to *Imma* (Nelmes et al 1996) at still higher pressure. There is a much larger stability region of β-tin and *Imma* stability compared to silicon, probably due to effects of the 3d core electrons (Vohra et al, 1986) before the Si-like sequence of simple hexagonal, *Cmca* (Ribiero and Cohen, 2000; Takemura et al, 2001; Mujica et al, 2001) [16] and hcp is resumed. As with silicon, calculations by Lewis and Cohen (1994) suggest that the *Imma* phase is more stable than β-tin at 0K and at all pressures. Since these calculations did not include finite temperature effects, it is plausible that β-tin is stabilised only by entropy effects.

Like silicon, β-tin phase germanium does not return to diamond on depressurisation, forming instead another distorted tetrahedrally coordinated structure, ST12. Calculation shows ST12 to be a metastable phase, but more stable than BC8. However, on fast depressurisation the β-tin phase transforms to BC8. As with silicon, the BC8 phase can also decomposes to yet another metastable phase: the experimental data for this phase is quite poor, but the most likely candidate seems to be the randomly stacked tetrahedral phase as observed in heated, depressurised Si (Nelmes et al 1993).

4. Tin

Tin is unusual in that its metal-insulator transition can be induced by temperature change at ambient pressure as well as pressure increase at low temperature. At low temperatures, the low pressure crystal structures are essentially the same as silicon and germanium, diamond (semiconducting) and β-tin (metallic). At higher pressures between 9.5 and 50GPa (Barnett et al 1966, Olijnyk and Holzapfel, 1984) a tetragonal distortion of the bcc structure (bct) has been reported (Desgreniers et al 1989), above which the bcc structure is adopted.

The c/a ratio of bct tin varies from 0.91 to 0.95 with increasing pressure across its stability region, before jumping discontinuously to 1 (bcc). This is consistent with calculations by Cheong and Chang (1991), who show that a graph of energy of bct against c/a has a double minimum structure (one minimum being bcc).

The effect of phonon entropy in stabilising the high temperature phase β-tin has been shown theoretically by Pavone et al (1998).

5. Lead

Although it is a Group IV element, lead shows none of the structural behaviour of Si, Ge and Sn. The difference between lead and the other group IV elements arises from the overlap of the various electronic bands which does not allow a distinct sp^3 bonding without mixing with other bands. Lead is metallic and close packed (fcc) under ambient conditions, and goes through a series of phase transitions fcc $\rightarrow$ hcp $\rightarrow$ bcc with increasing pressure. There is no experimental evidence for a bct distortion of the bcc phase, as observed in tin.

Calculations of these structures show a similar sequence at 0K (Liu et al 1991). Swift (1999) has carried out ab initio calculations for phonons in all three phases. Using these in the quasiharmonic approximation he was able to determine the temperature dependence of the phase boundaries from first principles.

C. III-V compounds

1. Boron Nitride

Boron nitride resembles carbon, forming two graphitic polymorphs (rhombohedral and hexagonal) and two diamondlike ones (zincblende and wurtzite structures) which are increasingly stable at higher pressure. Ueno et al (1992) report a transition from the rhombohedral form to zincblende between 8 and 20GPa. No phase transition has been reported for either of the high pressure phases at pressures up to 100GPa, and theoretical estimates suggest the stability limit of zincblende BN may be above 1000GPa (Wentzcovitch et al 1987; Perlin et al, 1993). Like diamond, zincblende BN is exceptionally hard with a bulk modulus close to 400GPa (Vancamp and Vandoren, 1989; Knittle et al, 1989)

2. Boron Phosphide

Boron phosphide has the zincblende structure which is reported to be stable up to 110 GPa(Xia et al, 1993). Calculations also suggested that the zincblende structure would become unstable with respect to rocksalt between 139 and 160GPa (Wentzkovitch et al, 1987; Van Camp and Van Doren, (1993); Kocinski and Zbroszczyok (1995) but this has yet to be confirmed experimentally. The experimentally determined bulk modulus was found to be lower than that predicted by *ab initio* pseudopotential calculations by Cohen (1985).

[16] this was previously reported as having double-hexagonal stacking

3. Boron Arsenide

BAs has been found experimentally to undergo a collapse from the zincblende to an amorphous structure at 125GPa (Greene et al., 1994), which persisted on increasing pressure and on depressurisation back to ambient. Previously, total energy calculations on a limited range of structures (Wentzkovitch et al, 1987) had found that BAs became unstable with respect to rocksalt at a similar pressure.

4. Boron Antimonide

Boron antimonide has yet to be synthesized experimentally: the zincblende structure is chemically unstable at ambient, but it is possible that it might be stabilised at higher pressure.

5. Aluminium Nitride

Aluminium nitride has the wurtzite structure, transforming to rocksalt at pressures reported as 14-20GPa (Xia et al, 1993) and 23GPa (Ueno et al, 1994). There are no further reported transitions.

The transition is not reversible, samples retain the rocksalt structure down to ambient. In a combined high-T high-P study Vollstadt et al (1990) found that rocksalt was obtained on quenching from 1900K and 16.5GPa.

Both experiments and calculations (Christiansen and Gorczyca 1993) show that the effect of pressure on the wurtzite structure is to reduce the c/a ratio further away from its ideal value.

6. Aluminium Phosphide

AlP is unstable in moist air, emitting poisonous phosphine gas, which has inhibited experimental studies of its high pressure structures. The zincblende phase forms grey or yellow crystals. There is a metallisation phase transition at around 15GPa, but the high pressure phase is uncertain. The most likely candidate is the NiAs structure (Greene et al, 1994). The transition is reversible, with a hysteresis of about 10GPa.

Early total energy calculations considered only the rocksalt structure (Zhang and Cohen, 1989) which is ruled out by the diffraction patterns, but more recently Vancamp and Vandoren (1995) and Mujica *et al* (1999) have predicted a series of transitions zincblende → (7.7GPa) NiAs → (52GPa) $Cmcm$ → (∼100GPa) CsCl.

7. Aluminium Arsenide

AlAs has technological importance in forming epitaxial multilayer structures with GaAs, with which it is closely lattice-matched. It is also poisonous. The metallisation transition has been observed at 12.4 GPa in bulklike thin films by Raman spectroscopy (Venkateswaran, 1992), microscopy (Weinstein et al , 1987) and X-ray diffraction Greene et al, 1994). The resulting NiAs structure is the only known high pressure phase to 46GPa. The transition is reversible, with a hysteresis of about 10GPa.

Calculations by Mujica et al (1999) suggest that the sequence of transitions is zincblende →(7GPa) NiAs →(36GPa) $Cmcm$ → (∼ 100GPa) CsCl

8. Aluminium Antimonide

AlSb has a metallisation transition at around 8GPa, and the most likely identity of the high pressure phase is $Cmcm$ (Nelmes et al 1997). Previous energy dispersive crystallography (Baublitz and Ruoff, 1983, Greene et al 1995) had suggested a β-tin structure, which was subsequently shown by total energy calculation to be energetically unstable with respect to NiAs (Rodriguez-Hernandez et al, 1996), demonstrating that β-tin is *not* the stable phase, but not confirming that NiAs is. More recent calculation (Mujica et al, 1999) showed that the $Cmcm$ structure is more stable, and suggested a sequence zincblende → (4.7GPa) $Cmcm$ → (50GPa) CsCl. Unfortunately, the $Cmcm$ phase does not fit the experimentally observed diffraction pattern (Nelmes and McMahon, 1998), so it is likely that a still more stable phase exists.

A further phase transition was noted experimentally at 41GPa (Greene et al, 1995) but the diffraction pattern was very poorly resolved and its structure remains unresolved experimentally. Thus it is not clear whether it is the CsCl phase or some more complex phase which Mujica et al (1999) did not consider.

9. Gallium Nitride

GaN forms a wurtzite structure at ambient, transforming to NaCl at about 37GPa. (Xia et al, 1993). This transition is reversible with a hysteresis of about 20GPa. Experiments have been conducted up to 70GPa and no further phase transitions have been identified.

Total energy calculations on GaN using either LMTO (Gorczyca and Christensen, 1991, Christiansen and Gorczyca, 1994) or pseudopotentials and plane waves (Vancamp et al, 1992 and Munoz and Kunc, 1993) reproduce the transition but predict phase transition pressures

higher than those found experimentally. Comparison between all electron Hartree-Fock and DFT calculations (Pandey et al, 1994, 1996) gave similar results.

Unlike other nitrides, the axial ratio of wurtzite GaN is not reported to change with pressure(Ueno et al. 1994)

10. Gallium Phosphide

Gallium phosphide metallises at around 23GPa, and the experimental evidence (Nelmes, 1997, and data from Baublitz and Ruoff 1982) is that the high pressure phase is disordered *Cmcm*. Total energy calculations show the importance of the 3d electrons, (Garcia and Cohen , 1993) and suggest (Mujica and Needs, 1997) that the SC16 phase should be stable between 14.7GPa and 20.3GPa, beyond which the β-tin phase is stabilised. In view of the kinetic difficulties in obtaining SC16, and observed amorphisation (Itie, 1993 but not Hu, 1984) on depressurisation, the thermodynamic stability of that structure seems likely despite the lack of experimental evidence. The calculations predict further transitions to *Immm* at 38.8GPa and ultimately to CsCl above 250GPa.

11. Gallium Arsenide

Gallium arsenide, a direct bandgap semiconductor, has long appeared to be the most promising of the III-V compounds for device applications. Perhaps because of this, it is also one of the most studied. At ambient temperature, its phase transitions tend to be sluggish and the diffraction patterns of the high pressure phases characterised by broad peaks indicative of strain and disorder, while the similar scattering power of Ga and As made determination of site ordering a challenging task. Much of the early experimental and theoretical work was inconsistent, but more recently a consistent picture has emerged thanks to annealing of pressurised samples to improve the quality of the diffraction pattern and overcome transition barriers between metastable structures.

Under ambient conditions and up to 13GPa, GaAs adopts the zincblende structure. Thermodynamically, there is a small range of stability of the SC16 phase, to about 14.5GPa. At higher pressures (Besson 1991, Crain et al 1994, Mujica and Needs 1996, Kelsey et al 1998) it adopts a site-ordered *Cmcm* structure (Nelmes and McMahon, 1998) which remains stable up to at least 108GPa (Weir et al 1989).

This simple picture of thermodynamically stable phases is complicated by a plethora of observed metastable phases. The SC16 phase, apparently thermodynamically stable, appears to be inaccessible from ambient pressure, having been made experimentally only by heating at pressure (McMahon et al 1998). Once formed, SC16 has a large range of room temperature metastability from ambient to 20GPa, but a much narrower range of true stability is inferred from total energy calculations and temperature cycling experiments (Crain et al 1994, McMahon et al 1998). On depressurisation of the *Cmcm* phase, a metastable, tetrahedrally coordinated, cinnabar structure is obtained: calculations suggest that this structure has no range of equilibrium stability (Kelsey et al, 1998, Mujica et al, 1998)

12. Gallium Antimonide

In recent work McMahon et al (1994) report that GaSb transforms from zincblende to an *Imma* phase at 7GPa This is a small distortion from the β-tin previously reported by Jamieson (1963) Yu et al (1978) and Weir et al (1987). Due to the absence of the (110) and (310) diffraction peaks the structure is assumed to be disordered.

Under further pressure the *Imma* distortion is increased away from 'ideal' β-tin (a=b, $\Delta = \frac{1}{4}$) toward 'ideal' simple hexagonal (b=c $\Delta = \frac{1}{2}$). A further transition was reported by Weir et al at around 61GPa - McMahon et al (1994) found a similar transition starting at 63 GPa which was ascribed to a body centred cubic structure.

It is curious that GaSb appears to be the only III-V compound with a thermodynamically stable site disordered structure at room temperature[17] : this may result from its lower ionicity than other III-V compounds, but it will still be of interest to examine whether it exhibits an order-disorder transition at low temperature.

13. Indium Nitride

InN adopts the wurtzite structure at ambient conditions, transforming to a rocksalt structure at higher pressure. Although there is some uncertainty about the transition pressure, recent experiments suggest transition pressures around 12GPa (Ueno et al 1993,1994, Xia et al 1994).

There is a structural signature of wurtzite instability observed both experimentally and in calculations: the c/a ratio increases between 10 and 16GPa, indicative of

[17]It is possible that the *Cmcm* phase of GaP is also disordered, although calculations and experiment disagree and the stability of SC16 makes it less clear.

an incipient elastic instability. (Bellaiche and Besson, 1996, Besson et al 1996)

Total energy calculations have shed little further light on the situation, transition pressures being reported at 25.4GPa (Perlin, 1993) and 4.9GPa (Munoz and Kunc, 1993). The large discrepancy between calculated and experimental values for the transition pressure in the pseudopotential calculations of Perlin et al (1993) may result from their adoption of the ideal axial ratio for wurtzite

Experiments have been conducted up to 35GPa (Xia et al, 1994) without any further phase transitions being observed.

14. Indium Phosphide

InP transforms from zincblende to rocksalt at around 10GPa (Minomura and Drickhamer 1962, Jamesson, 1963) with a further continuous change (Menoni and Spain, 1987) to *Cmcm* 28GPa (Nelmes et al, 1997). Ab initio calculation by Mujica and Needs (1997) confirm this trend (with transition pressures about half those reported experimentally), and further predict transitions to *Immm* at 50GPa and CsCl at 102GPa.

15. Indium Arsenide

InAs appears to behave similarly to InP. It has been reported to transform from zincblende to rocksalt at 7GPa and then via an intermediary to *Cmcm*. (Vohra et al 1985, Nelmes et al 1995) As discussed by Nelmes et al (1998), there is considerable uncertainty about the correct interpretation of the data and it is likely that these phases are somewhat distorted.

Total energy calculations by Christensen (1986) and by Mujica and Needs (1997) find NaCl, *Cmcm* and *Immm* to be very close in energy at high pressure, predicting transformations ZB-NaCl (3.9GPa) NaCl-*Cmcm* ("between 3.0 and 4.5GPa") and *Cmcm*-*Immm* (24GPa). This latter transition has not yet been observed in experiments up to 46GPa. Distinguishing between these phases is very close to the resolution of current total energy methods.

16. Indium Antimonide

Like gallium arsenide, crystallography in InSb is made more difficult by the similar scattering power of the two atoms. However, this problem has been largely circumvented by using synchrotron radiation at a frequency close to the In K-absorbtion edge which greatly enhances the contrast. A huge amount of work has been done on InSb, much of it rendered obsolete by later more accurate studies, (Nelmes et al, 1993, Nelmes and McMahon, 1995, Mezouar et al (1996) Nelmes and McMahon, 1996) and here only the currently accepted structures, observed experimentally and confirmed by total energy calculation, are described.

The ambient structure is zincblende, and on pressurisation above 2GPa there is a transformation to the so-called super-*Cmcm* phase. This phase is a site-ordered decoration of the simple hexagonal lattice with 24 atoms in the unit cell. At higher temperatures, and at higher pressures, this delicate ordering breaks down and the crystal structure reverts to a simple *Immm* symmetry. At 21 GPa a final transition to a disordered bcc phase occurs.

Again, metastability plays a role. Total energy calculations have shown a range of different structures to be extremely close in energy (Guo et al 1993, Kelsey, 1997), and it is no surprise that each transition occurs via distinctive metastable intermediate phases. Moreover, similarity in energy between the various decorations of the hexagonal lattice leads to low order-disorder transition temperatures, and the slow growth by high pressure recrystallization of the super-*Cmcm* phase. On depressurisation back to ambient the β-tin phase is recovered (Darnell and Libby, 1963) which may develop a small orthorhombic distortion (Nelmes et al 1993): β-tin also appears as an intermediate phase during the growth of super-*Cmcm*.

VI. TRANSFORMATION MECHANISMS

A. Elastic Stability

Despite the accuracy with which *ab initio* electronic structure methods have been able to describe the energetics of pressure response in complex solids there remains little known about the mechanical origin of the prototypical reconstructive phase transition between the fourfold- and sixfold-coordinated structures. The essential question is as follows: How can hydrostatic compression of a cubic structure give rise to a phase transition to a tetragonal or orthorhombic structure?

The usual Born description for the stability of a cubic crystal is expressed in terms of elastic constants as follows (See for example, Born and Huang, 1956)

$$B_T = (C_{11} + 2C_{12})/3 > 0 \quad (3)$$

$$C_{44} > 0 \quad (4)$$

$$C' = (C_{11} - C_{12})/2 > 0 \quad (5)$$

where C_{ij} are the conventional elastic constants and B_T is the bulk modulus. The quantities C_{44} and C' are the shear and tetragonal moduli of a cubic crystal. These conditions are known as the spinodal, shear and Born criteria respectively. Similar criteria hold for non-cubic materials

Wang et al (1993), showed that under external pressure these relations need to be modified to decribe changes in enthalpy rather than energy. Their stress-strain relations involve the *elastic stiffness tensor* $B_{ijkl}(\mathbf{X}) = \partial\sigma_{\mathbf{ij}}/\partial\eta_{\mathbf{kl}}(\mathbf{x})$. Where σ_{ij} is the applied stress and η_{kl} is the strain defined with respect to finite strain (Lagrange) coordinates. X and x are then the coordinates before and after the deformation.

When deformation is expressed in terms of Lagrangian strain the new stability criteria for crystals under hydrostatic pressure are

$$\tilde{B}_T = (B_{11} + 2B_{12})/3 > 0 \quad (6)$$

$$\tilde{G} = B_{44} > 0 \quad (7)$$

$$\tilde{G}' = (B_{11} - B_{12})/2 > 0 \quad (8)$$

where the elastic stiffness constants are defined by $B_{11} = C_{11} - P$, $B_{12} = C_{12} + P$, $B_{44} = C_{44} - P$ and $P = -\partial U/\partial V$.

Mizushima et al (1994) have considered the the diamond $\rightarrow$ β-tin transformation in silicon using these criteria and calculated stiffness constants, using DFT for static calculation and a Tersoff (1988) potential for molecular dynamics. Their results suggest that while no transition is expected on the basis of the Born criteria, the revised stability condition $\tilde{G}' > 0$ is violated. Their predicted transition pressure is substantially higher than either observed experimentally or predicted on the basis of thermodynamic criteria, suggesting that simple tetragonal shear is not the transformation mechanism in this case.

These are kinetic criteria, under which the structure becomes mechanically unstable, as opposed to thermodynamic instability used in total energy calculations which makes no reference to a transition route. The resulting thermodynamic transition pressure will be a *lower* limit to the observed transition. By contrast, the elastic criteria prescribe a particular homogeneous deformation as the reaction path - the real path is probably more complex, hence elastic criteria give an upper limit on the transition pressure.

In other materials these new criteria have been shown to correspond exactly to the transition (Karki et al , 1997)

B. Landau Theory

The Landau theory of phase transitions can be applied to structural transitions between any two phases where the symmetry of one phase is a subgroup of the other. The general approach involves an expansion of the free energy F as a power series in an order parameter u:

$$F(u) = F_0 + A_2u^2 + A_3u^3 + A_4u^4 + ... \quad (9)$$

The order parameter corresponding to minimum free energy is zero in the high-symmetry phase ($A_2 > 0$) while it is nonzero in the low symmetry phase ($A_2 < 0$).

In its usual application, the A_i are functions of temperature. It is also possible to apply the theory in the case where the A_i are pressure dependent.

Many of the transitions discussed in this review satisfy the symmetry-breaking subgroup condition. A much studied example is the diamond to β-tin transition in which the cubic-tetragonal symmetry change is from O_h^7 to D_{4h}^{19}

To actually apply the Landau theory, the order parameter must also be specified. This requires knowledge (or assumption) about the actual mechanism of the phase transition. Hebbache (1994) has applied the theory using tetragonal shear as the order parameter linking diamond and β-tin. although this postulated route probably does not correspond to the path actually taken in the real material.

If the driving force for the transition is purely pressure, the A_2 parameter becomes the (pressure dependent) elastic constant associated with tetragonal shear.

The BC8 $\rightarrow$ R8, β-tin $\rightarrow$ $Imm2$ (or $Imma$) and $Immm$ - $Imma$ transitions are also candidates for the Landau treatment, although in each of these cases the driving force for the transition is a combination of temperature and pressure.

General schemes for combining Landau theory and first principles calculations have been put forward and applied to high-pressure structural transitions in perovskites by Warren (1995) and in cesium halides by Nardelli *et al* (1995). Their application to III-V systems is a promising area for further work.

C. Soft phonon modes

Sometimes, the order parameter for a transformation can be related to a particular normal mode of a system. In such cases, lowering of the frequency of the phonons associated with this mode (the soft phonon mode) can indicate an upcoming phase transition. In a truly second order transition, the phonon frequency would go to zero, but more commonly the transition involves both the vibrational mode and an elastic modulus and the phonon frequency remains non-zero.

Phonon frequencies can be measured experimentally via inelastic neutron scattering for the whole spectrum, or Raman or infrared spectroscopy for the Γ-point phonons which are often the soft modes. They are also tractable to calculation, hence phonon softening is a powerful tool for studying both the possibility and the mechanism of a phase transition.

A simple example of a displacive transition operating by a phonon mode coupled to an elastic instability is the transition from the β-tin phase to the simple hexagonal

by displacement of one of the two body-centred tetragonal sublattices in the c-axis direction. This displacement pattern is equivalent to a zone-centre LO phonon mode of the β-tin structure coupled to a strain which, in a rigid rod picture, would not require any change of near neighbour bondlengths (Ackland, 1994). Using DFT, Needs and Martin (1984) and Chang and Cohen(1985) have investigated this transformation path for silicon, finding a softening of the phonon mode with increasing pressure. They suggest that this is likely to be the transformation mechanism - moreover, the same LO phonon path also enables the transition to the $Imma$ which had not yet been reported when the work was carried out.

In binary compounds a similar transition occurs between β-tin, $Imm2$ and $Immm$. These phases have all been reported to occur metastably in InSb, and DFT calculation by Kelsey and Ackland (2000) have followed this path finding no barrier and the end points to be extremely close in energy, suggesting that the observed structure might be determined by anisotropic stresses in the sample.

Experimentally, in-situ Raman spectroscopy of pressure-induced mode softening in metallic phases is difficult because of weak signals and small sample size. Olijnyk (1992) has carried out Raman experiments on high-pressure silicon, studying both the LO and TO zone centre optical modes of the β-tin lattice. The frequency of the TO mode of the β-tin phase was found to increase with pressure while that of the LO branch decreased and broadened. This is in agreement with the results of *ab initio* simulations (Chang and Cohen, 1986): the broadening suggests a large amplitude for the atomic vibration as the mode approaches instability, consistent with the Landau picture.

In germanium the frequencies of both the TO and LO phonons of the β-tin structure initially increase: consistent with the larger range of stability of its β-tin phase.

The $Imma$ phase, observed in both Si and Ge at pressures between β-tin and simple hexagonal, can be related to these structures via the same phonon mechanism.

Transitions occurring via a soft phonon mode or elastic instability may be martensitic in nature. If so, the orientation of the high pressure phase will be related to that of the low pressure phases (typically, a number of twin *variants* are formed). X-ray diffraction studies using single crystals taken through the transition should show strong preferred orientation effects in the high pressure phase, observable on an area detector. These could be used to deduce the transformation mechanism.

The report of a possible second order phase transition in InP (experiment by Nelmes et al 1997, calculation by Mujica and Needs, 1997) arising essentially from a soft phonon mode in the rocksalt structure lowering the symmetry to $Cmcm$, suggests that measurement of the phonon spectrum of InP would be interesting.

Very recently, Zunger et al (2001) carried out an examination of phonon instabilities in NaCl, β-tin and CsCl structure across the full range of binary semiconductors, with a view to predicting which distortions would be observed in practice.

D. Order-disorder transitions and associated symmetry breaking

The β-tin structure has an unusual topology, having four nearest neighbours, and two more close by. As discussed by Nelmes et al (1997) there is no experimental evidence for ordering of species in binary compounds which form a β-tin lattice. In fact, this conclusion is drawn from the absence of a (110) 'difference' peak arising from ordering in which all four nearest neighbours of a given atom are of different species to it: other orderings might be possible, but in many cases these are ruled out on energetic considerations by ab initio calculation which show the simplest ordering to be favoured[18].

An alternative possibility is that the observed disorder is a kinetic effect, arising simply from the slow diffusion of atoms into their ordered position. Support for this comes from the large hysteresis in the zincblende-β-tin transformation, which transformation is driven primarily by the large volume collapse rather than any subtle ordering effects.

Alternately, β-tin the structure may undergo an order-disorder transition like those observed in metallic alloys. Here, the disordered phase is stabilised at high temperature by its larger configurational entropy. Simple Bethe and Bragg-Williams models, developed in the context of intermetallic alloys, can be applied. These based on the idea of nearest and next nearest neighbour bond-strengths. Numerical simulation of these processes reduces to an Ising model with second neighbour interactions: for the β-tin lattice this model (Ackland, 2001) gives a disordered high temperature phase and can give either the ordered structure or a spin glass at low temperature.

E. Finite size effects and microindentation

High pressure phase transitions can be induced by uniaxial compression (point loading) and characterised using atomic force microscopy. Mann et al, (2000) reported

[18] there is some evidence for short range order from XAFS experiments, Van Petighem, private communication

seeing amorphous, BC8 and R8 silicon depending on the size of the indentation.

Planar or linear defects, such as inversion domain boundaries (Crain et al, 1993) and phasons (Dmitrenko et al, 1999) do not contribute to the extensive free energy, however for a finite crystal their entropic contribution may be large enough to make a disordered structure the stable phase (Bruce et al, 2000). Consequently, some crystal structures are only stable against spontaneous defect formation once they reach a critical size.

VII. VIBRATIONAL PROPERTIES

The phonon behaviour of the III-V and group IV materials has been studied over a large number of years. We concentrate here on the pressure dependence, which is best described by mode-specific Gruneisen parameters $\gamma_i = \partial(\ln \omega_i)/\partial \ln V$. For the diamond/zincblende structures the transverse acoustic (TA) modes have negative γ_i in most cases, carbon being a notable exception. Most studies using two-photon Raman scattering looked only at zone boundary modes (Weinstein and Piermarini, 1975; Weinstein, 1977; Trommer et al 1976; Grimsditch et al 1978; Yu and Welber,1978; Parsons, 1977; Trommer et al 1980; Olego and Cardona 1982).

More recently, inelastic neutron scattering has studied dispersion along entire phonon branches (Klotz et al. 1995,1997), and confirmed the trends toward softening with pressure hold for entire branches.

There have been a number of efforts to find a simple relation between the TA(X) mode Gruneisen parameter and the transition pressure, but with limited success (Weinstein, 1977, Arora, 1990): it appears that while the TA(X) phonon is related to the transition, the actual mechanism is more complex than a single phonon softening.

Theoretically, the TA mode softening can be qualitatively understood by simple rigid-ion lattice dynamics (Talwar and Vandevyver, 1990), who predicted that TA(L) would soften most in InP, GaSb and GaAs while TA(X) would soften more in GaP, InAs and InSb, however figure4 shows that these groupings do not have similar observed high pressure phases. TA phonons have been more accurately described by total energy calculations for softening in Si and Ge (Yin and Cohen, 1982) and hardening in C (Pavone et al, 1993). Measured and calculated results are given in table VII.

Experimental study of phonons in high pressure phases is still in its infancy, both sample size and conductivity being a problem, but with the number of theoretical predictions of mode softening, it is a potentially fruitful area.

VIII. THEORETICAL EQUILIBRIUM EQUATION OF STATES

A combination of phonon and structural calculation techniques can be used to evaluate complete equilibrium equations of states. In principle any method for evaluating the total energy will suffice, but in practice some ab initio method is likely to produce the best results.

The strategy is to evaluate the Gibbs free energy for all crystallographic phases at all pressures and temperatures. Static total energy calculations can be used to find the enthalpy as a function of volume - these are the calculations which have been discussed throughout the review which give a 0K equation of states[19].

To extend to higher temperatures, the quasiharmonic approach is used. The phonon dispersion relation must be evaluated using either linear response theory or lattice dynamics. One needs to calculate sufficient phonons to sample the entire Brilloiun zone at a range of possible cell volumes. For given pressure, temperature and volume, the free energy for the phase can now be evaluated:

$$G(P,V,T) = U_o(V) + PV - k_B T \ln Z(V,T)$$

Where U_o is the total energy calculated from the ideal crystal structure, and Z is the partition function:

$$Z(V,T) = \int_{BZ} \exp\left(\hbar\omega_{\mathbf{k}}/kT\right) d^3\omega_{\mathbf{k}}$$

where in practice the integral over the Brilloiun Zone (BZ) is carried out numerically. Some care has to be taken to avoid numerical instabilities for very long wavelength phonons $\mathbf{k} \to \infty$.

Assuming pressure and temperature to be the external variables (hydrostatic conditions), the free energy of a particular crystal structure at a particular temperature and pressure is found by minimising G(P,V,T) with respect to V[20]. The stable crystal structure is the one with minimum G(P,T). Other thermodynamic properties can also be determined from the partition function using standard statistical mechanics techniques. This methodology has been laid out in detail recently by e.g. Swift 1999 and applied *inter alia* to silicon and germanium through the diamond-β-tin transition GaalNagy et al (1999).

---

[19] strictly, even this is incorrect since zero-point phonons are excluded, but in practice the free energy differences between various phases arising from zero point vibrations are small

[20] strictly, the free energy minimisation should be carried out over all independent lattice and internal parameters, but in practice optimising the total energy with respect to these is sufficient

At higher pressures, or in the presence of unstable phonon modes, the quasiharmonic approximation breaks down and one has to include anharmonic effects. A simple way to do this is to use larger atomic displacements in calculating force constants. [21] For still greater accuracy in determining the exact position of the phase boundary, thermodynamic integration (Frenkel and Ladd, 1984) or biassed Monte Carlo methods (Bruce et al, 1997) may be needed to probe the free energy difference between two unrelated crystal structures exactly, while molecular dynamics may be the best way to investigate soft mode or melting transitions.

Under extremely high temperatures, Swift has considered the effects of thermal excitation of the electrons on the free energy. This effect does not seem to affect the free energy differences significantly.

IX. CONCLUSIONS

The study of high-pressure phases in III-V and Group IV semiconductors has now reached a natural plateau. Most of the cataloguing of structures experimentally is complete, and most structures seem to be solved. There are a few gaps at particularly high pressures, but it seems unlikely that anything very surprising will be found (with the possible exception of carbon). Moreover theoretical work, in particular the pseudopotential/plane wave implementation of density functional theory, has proved itself to be extremely reliable in describing the observed behaviour. Thus insofar as solving structures experimentally and understanding them theoretically the field is mature.

Apart from their structures very litle is known of other properties of these new high-pressure materials. Computer simulations indicate their metallic nature, and have suggested some will be superconducting, but their precise mechanical, chemical and optical properties remain unknown.

An area not touched on in this review is the behaviour of ternary mixtures of III-V materials, either as a true compound or grown artificially in multilayer structures. The alloying possibilities are enormous, and even at ambient deliberate design of ternaries is only now being considered (Wang et al, 1999). There is also a prospect of using high pressure to alloy or order compounds which would not mix at ambient, and then recover these mixtures to ambient.

The existence of metastable states points at another exciting and relatively untouched area, that of determining kinetics and transition paths. Mode softening and Raman spectroscopy shed some light on this, but direct probes of microstructure such as X-ray diffraction of former single crystals after the transition, and time-resolved crystallography are more likely to lead the way in the long run. The ultimate pay-off here is to understand how to use pressure treatment as an accessory to heat treatment in preparing materials with desirable microstructural properties. Computer simulation also has a role to play here, stepping beyond single unit cell total energy determination on to molecular dynamics, in determining transition paths and hence relating high pressure microstructure at the nanometre level to the initial crystal. Some examples of creating new, long-lived metastable states which can be recovered to ambient condition have been discussed here, and the prospect of using pressure in material processing is not too far off.

With all these possibilities, research in high pressure semiconductors may be about to move away from investigation and into design.

TABLE I. Properties of group IV elements: diamond lattice parameter, ambient bandgap, first transition pressure, volume collapse on metallisation, melting point. Thermodynamic data are taken from the CRC Handbook and other sources are given in the text.

	C	Si	Ge	α-Sn
a Å(ambient)	3.567	5.431	5.6579	6.49
ambient bandgap (eV)	5.5	1.11	0.67	0.1
P [dia-metal] (GPa)	4000	12	7	0
melting point		1693	1210	232 (β)

[21] This requires a series of force constant calculations at each volume, with the energy change linking the displacement to a temperature via $\Delta U = \frac{1}{2} k_B T$

TABLE II. Structural parameters for the *Cmcm* phase in III-V compounds.

	GaP	GaAs	InP
P (GPa)	20	20	28
a(Å)	4.707	4.971	4.879
b(Å)	4.949	5.272	5.088
c(Å)	4.701	4.779	4.923
y(III)	0.647	0.649	0.658
y(V)	0.159	0.166	0.143

TABLE III. Properties of B-V compounds: Zincblende lattice parameter, ambient bandgap, first transition pressure, volume collapse on metallisation, melting point. Thermodynamic data are taken from the CRC Handbook and other sources are given in the text.

	BN	BP	BAs
aÅ(ambient)	3.615	4.558	4.777
ambient bandgap (eV)	6.0	2.0	0.1
P [metal] (GPa)	4000	12	7
melting point		1693	1210

[a]

[a]All transition pressures are theoretical (Wentzkovitch et al 1987)

TABLE IV. Properties of Al-V compounds: Zincblende lattice parameter (wurtzite for AlN), ambient bandgap, first transition pressure, volume collapse on metallisation, melting point. Thermodynamic data are taken from the CRC Handbook and other sources are given in the text.

	AlN	AlP	AlAs	AlSb
a,c Å(ambient)	3.11,4.98	5.463	5.660	6.1355
ambient bandgap (eV)	6.3	2.4	2.2	1.6
P[metal] (GPa)	23	14	12.3	8
ΔV %	18%	17%	17%	15%
melting point	3000	2803	2013	1333

TABLE V. Properties of Ga-V compounds: Zincblende lattice parameter (wurtzite for GaN), ambient bandgap, first transition pressure, volume collapse on metallisation, melting point. Thermodynamic data are taken from the CRC Handbook and other sources are given in the text.

	GaN	GaP	GaAs	GaSb
a,c Å(ambient)	3.19,5.19	5.451	5.653	6.096
ambient bandgap	3.4	2.3	1.4	0.7
P[metal] (GPa)	37	22	17	8
ΔV %	18%	15.5%	17%	17%
melting point		1740	1511	983

TABLE VI. Properties of In-V compounds: Zincblende lattice parameter (wurtzite for InN), ambient bandgap, first transition pressure, volume collapse on metallisation, melting point. Thermodynamic data are taken from the CRC Handbook and other sources are given in the text.

	InN	InP	InAs	InSb
a (ZB, ambient)	3.545,5.703	5.869	6.058	6.479
ambient bandgap	2.05	1.4	0.4	0.2
P[metal] (GPa)	10	10	7	2
ΔV %	18-20%	16%	17%	20%
melting point		1335	1215	798

TABLE VII. Mode grüneisen parameters of several tetrahedral semiconductors at four different symmetry points of the Brillouin zone.

	TO(Γ)	LO(Γ)	TA(X)	TA(L)
GaP	1.09	0.95	-0.72	-0.81
GaAs	1.39	1.23	-1.62	-1.72
GaSb	1.23	1.21		
InP	1.44	1.24	-2.08	-2.00
Si	0.98	0.98	-1.4	-1.3
Ge	1.12	1.12		
C	0.98	0.98	0.4	

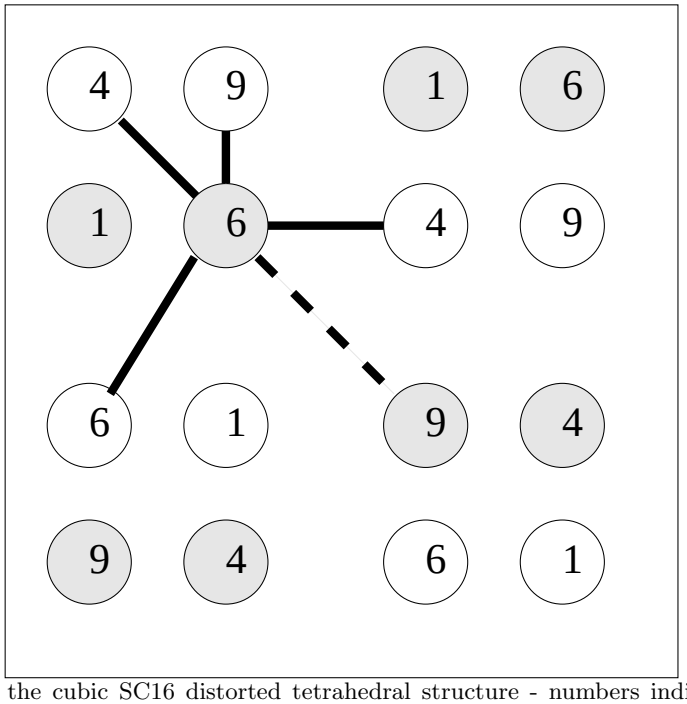

FIG. 1. Projection drawing of the cubic SC16 distorted tetrahedral structure - numbers indicate approximate height in c-direction, in tenths of the cell parameter (there are two free internal parameters defining the exact heights). Black and white circles represent different atomic species. Solid lines show the bonded neighbour of one of the atoms. The BC8 structure is similar, with all circles representing the same species and only one internal parameter required. The rhombohedral R8 structure is formed by breaking and remaking bonds along one of the body diagonals: the new bond formed in R8 is shown by the dashed line in the figure, with the diametrically opposite bond being broken. R8 requires two internal parameters, one for the four atoms along the rebonded body diagonal, and one for the remaining twelve atoms. The is no binary equivalent of R8, since the rebonding would entail forming like-species bonds.

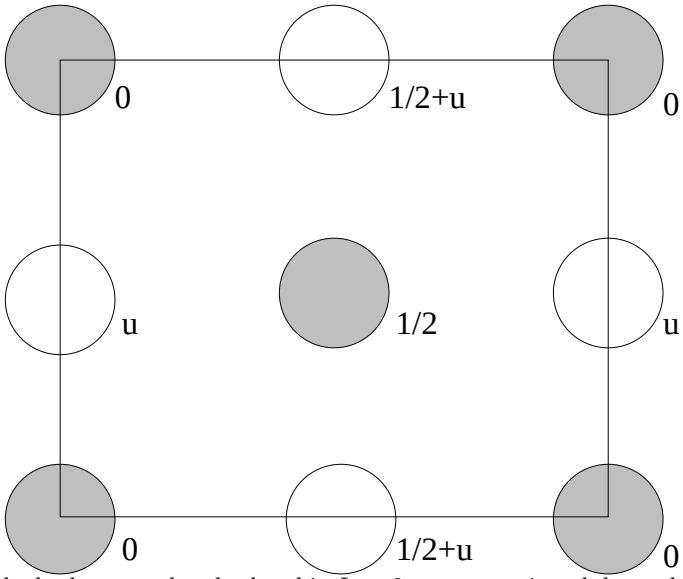

FIG. 2. Projection drawing of the body-centred orthorhombic $Imm2$ structure viewed down the c-axis. Grey and white circles represent atoms of different species Special cases of this include $Immm$ (u= 0.5), NaCl (u=0.5 and a=c=b/$\sqrt{2}$), β-tin (a=b, u=0.25) and zincblende (a=b=$\sqrt{2}c$, u=0.25).

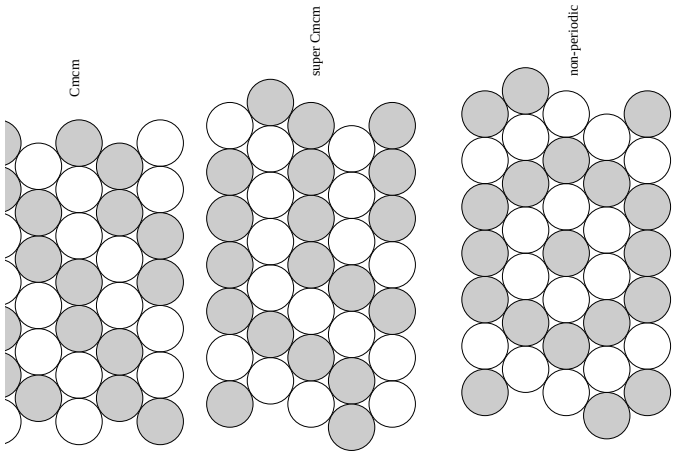

FIG. 3. Possible decorations of a simple hexagonal lattice giving rise to $Immm$, $Cmcm$ and super-$Cmcm$ structures (atom types alternate in subsequent layers perpendicular to the page), and to a non-periodic structure which has more than 4 unlike neighbors.

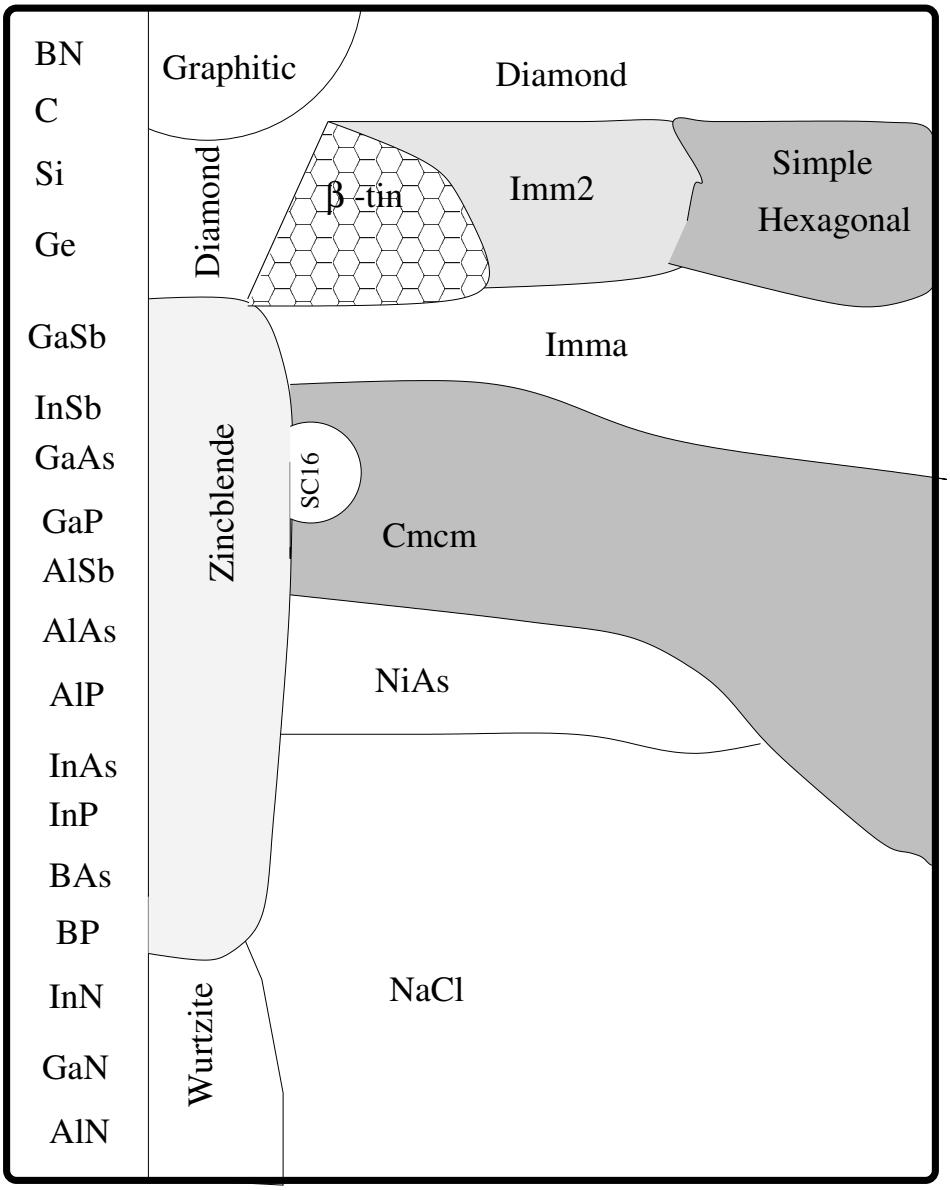

FIG. 4. Schematic diagram showing the observed and predicted structures for group IV and III-V semiconductors. Structures are explained in the text, the diagram incorporates both experimentally observed phases and theoretically predicted ones.

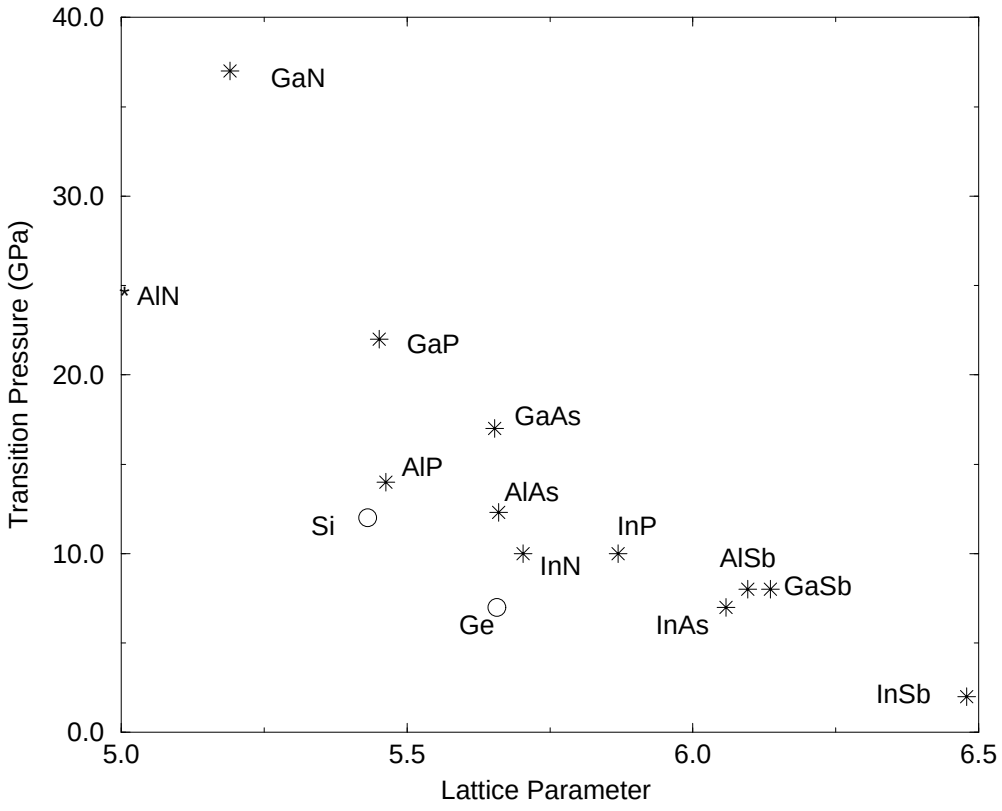

FIG. 5. Graph illustrating the correlation between lattice parameter in the ambient phase and transition pressure to the first metallic phase. Wurtzite structures (nitrides) are plotted against c lattice parameter. Theoretical predictions for carbon and boron compounds are omitted: they followed the same trend, but lie far above the top left corner of the figure.

REFERENCES

Ackland, G.J., 1991, Phys.Rev.B. **44**, 3900; 1989 Phys.Rev.B. **40**, 10351
Ackland, G.J., 1994, Phys.Rev.B. **50**, 7389.
Ackland,GJ Warren,MC and Clark,SJ, 1997 J.Phys.CM, **9**, 7861.
Ackland, G.J., 1998, Phys.Rev.Lett. **80**, 2233.
Ackland, G.J., 2001, Phys.Rev.Lett.
Ahuja,R, Eriksson,O, Johansson,B 1999 Phys. Rev.B. **60**, 14475
Akbarzadeh, H, Clark, SJ and Ackland, GJ 1993, J.Phys.CM **5**, 8065.
D.Alfe, G. A. de Wijs, G. Kresse and M. J. Gillan, International Journal of Quantum Chemistry, 77, 871, (2000)
Arora, A.K., 1990, J.Phys.Chem. Solids **51**, 373.
Balamane,H, Halicioglu,T, Tiller,WA Phys Rev B, 1992, **46**, 2250
Barnett,J.E., Bean,V.E.and Hall,H.T. J.Appl.Phys 37 875 (1966)

Baublitz, M., and Ruoff,A.L., 1982, J.Appl.Phys. **53**, 6179.
Baublitz, M., and Ruoff,A.L., 1982, J.Appl.Phys. **53**, 5669.
Baublitz, M., and Ruoff,A.L., 1983, J.Appl.Phys. **54**, 2109.
Bellaiche,L., Kunc,K., Besson,J.M. Phys.Rev B, 1996, **54**, 8945
Bell,P.M., Xu, J.A. and Mao,H.K. in *Shock Waves in Condensed Matter* ed. Gupta,Y.M. (Plenum, NY) 1986, p124.
Belmonte,SA 1997, PhD thesis, University of Edinburgh.
Bernasconi, M., Chiarotti,G.L., Focher,P. Scandolo,S. Tosatti,E. and Parrinello,M. 1995, J.Phys.Chem.Solids **56**, 501.
Besson, JM, Mokhtari,EH, Gonzales,J and Weill,G, 1987 Phys.Rev.Lett **59** 473.
Besson, J.M., Itie,JP Polian,A Weill,G Mansot,JL and Gonzalez,J 1991, Phys.Rev.B. **44**, 4214.
Besson,J.M., Bellaiche,L. and Kunc,K. Physica Status Solidi B, 1996, **198**, 469
Bethe,H 1934 Proc.Roy.Soc.A, **145**, 699.
Biswas R., Martin R.M., Needs R.J., and Neilsen O.H., 1987 Phys.Rev.B. **35**, 9559.
Born M., and Huang K., *Dynamical Theory of Crystal Lattices* (Clarendon, Oxford, 1956).
Bruce,AD, Wilding,NB and Ackland,GJ Phys.Rev.Letters, 1997, **79**, 3002
Bruce,AD, Jackson,AN, Ackland,GJ and Wilding,NB Phys.Rev.E, 2000, **61**, 906; see also Ackland GJ, Wilding,NB and Bruce,AD MRS Symp.Proc. 499 (1997).
Car,R and Parrinello,M, Phys.Rev.Lett. **55**, 2471 (1985)
Carlone C., Olego D., Jayaraman A., and Cardona M., 1980, Phys.Rev.B **22**, 3877.
Ceperley,DM Alder,BJ (1980) Phys.Rev.Lett. **45**
Cernik,RJ, Clark,SM, Deacon,AM, Hall,CJ, Pattison,P, Nelmes,RJ, Hatton,PD, McMahon,MI Phase Transitions, 1992, **39**, 187
Chang, K.J., and Cohen,M.L., 1985, Phys.Rev.B. **31**, 7819.
Chelikowsky, J.R., 1987, Phys.Rev.B. **35**, 1174.
Chervin,JC, Canny,B, Besson,JM, and Pruzan,P Review of Sci.Inst., 1995, **66**, 2595
Christensen, N.E., 1986, Phys.Rev.B. **33**, 5096.
Christensen, N.E., 1998, Semiconductors and semimetals, **54** 49.
Christiansen,NE and Gorczyca,I. 1993 Phys.Rev.B **47** 4307.
Christiansen,NE and Gorczyca,I. 1994 Phys.Rev.B **50** 4397.
Clark,SJ, Ackland,GJ, Crain,J Phys Rev B, 1994, **49** 5341
Clark,SJ, Ackland,GJ and Crain,J.. Phys.Rev.B 52, 15035 (1995)
Clark,SJ, Ackland,GJ and Crain,J. Phys.Rev.B 55, 14059 (1997)
Clark,SJ, Ackland,GJ Crain,J. and Payne,M.C. Phys.Rev.B, 50, 5728 (1994)
Cohen, M.L., 1985, Phys.Rev.B. **32**, 7988.
Crain, J., Ackland,GJ and Clark,SJ 1995, Rep. Prog.Phys. **58**, 705.
Crain, J., Ackland,GJ, Maclean,J.R., Piltz,R.O. Hatton,P.D. and Pawley,G.S. 1994, Phys. Rev. B **50**, 13043.
Crain, J., Ackland,GJ, Piltz,R.O., Hatton,P.D. 1993, Phys. Rev. Lett. 70, 814.
Crain, J., Piltz,R.O., Ackland,G.J., Payne,M.C., Milman,V. Lin,J.S. Hatton,P.D., Nam,Y.H. and Clark,S.J. 1994, Phys. Rev. B. **50**, 8389.
Crain, J., Clark,S.J., Ackland,G.J., Payne,M.C. Milman,V. Hatton,P.D. and Reid,B.J. 1995, Phys. Rev. B. **49**, 5329.
Darnell, AJ amd Libby, WF 1963, Science, **139**, 1301.
Decker,D. 1971, J.Appl.Phys **42**, 3239.
Devreese, J.T., and Van Camp,P. (Editors), Electronic Structure, Dynamics, and Quantum Structural Properties of Condensed Matter. NATO ASI series, **21**.
Dmitrienko,VE, Kleman,M, and Mauri,F Phys.Rev.B, 1999, **60**, 9383
Dmitrienko,VE, and Kleman,M Phil.Mag.Letters, 1999, **79**, 359
Duclos,S.J, Vohra,Y.K. and Ruoff,A.L. 1990, Phys. Rev. B., **41**, 12021.
Dunstan,DJ and Spain, I. L., 1989, J. Phys. E **22**, 913.
Eremets,MI, Gauthier,M, Polian,A, Chervin,JC, Besson,JM, Dubitskii,GA, Semenova,YY Phys.Rev.B, 1995, **52**, 8854
Ernzerhof,M, Perdew,JP, and Burke,K Topics in Current Chemistry, 1996, **180**, 1
Fabian,J and Allen,PB Phys.Rev.Lett, 1997, **79**, pp.1885
Fahy S., and Louie S.G., 1987, Phys. Rev. B, **36** 3373.
Focher, P., Chiarotti, G.L. Bernasconi,M. Tosatti,E. and Parrinello,M. 1994, Europhys. Lett. **26**, 345.
Frenkel,D and Ladd,AJC, 1984 J. Chem. Phys **81** 188 .
Froyen, S., and Cohen,M.L., 1982, Solid State Commun. **43**, 447.
Froyen, S., and Cohen,M.L., 1983, Phys. Rev. B. **28**, 3258.
GaalNagy,K, Bauer,A, Schmitt,M, Karch,K, Pavone,P, Strauch,D Phys.Stat.Solidi B, 1999, **211,** 275-
Galli,G, Martin,RM, Car,R, Parrinello,M 1990, Science, **250** 1547
Garcia, A., and Cohen,M.L. , 1993, Phys. Rev. B. **47**, 4215.
Garcia, A., and Cohen,M.L. , 1993, Phys. Rev. B. **47**, 6751.
Giannozzi P., Degironcoli S., Pavone P., and Baroni S., 1991 Phys. Rev. B. **43**, 7231.

Gorczyca, I., and Christensen, N.E. 1991, Solid State Commun. **80**, 335.
Greene,RG, Luo,H. and Ruoff,AL, 1994 J.Appl.Phys. **76** 7296
Greene,RG, Luo,H. Ruoff,AL Trail,SS and Disalvo, JT, 1994 Phys.Rev.Lett **73** 2476.
Greene,RG, Luo,H. Ghamdehari,F. and Ruoff,AL, 1995 J.Phys.Chem.Solids **56** 517.
Greene,RG, Luo,H. Li,T. and Ruoff,AL, 1994 Phys.Rev.Lett **72** 2045.
Grimsditch, M.H., Anastassakis,E and Cardona,M., 1978, Phys.Rev.B **18** 901.
Grumbach,M.P. and Martin,R.M., 1996, Phys.Rev.B **54**, 15730.
Guo,G.Y., Crain,J. Blaha,P. and Temmerman,W.M. 1993, Phys. Rev. B. 1993 **47**, 4841.
Hanfland,M, Schwarz,U, Syassen,K, Takemura,K Phys Rev Letters, 1999, **82**, 1197
Hebbache, M., 1994, Phys. Rev. B. **50**, 6522.
Hemley,R.J. and Ashcroft, N.W., Physics Today, 1998, **51**, 26.
Hohenberg,P and Kohn,W 1964, Phys Rev. **136** B864
Hu,J.Z, Black, D.R. and Spain, I.L. 1984, Solid State Comm. 51 285
Hu,J.Z, Merkle,L.D., Menoni,C.S. and Spain, I.L. 1986, Phys. Rev. B. **34**, 4679.
Hull,S and Keen, D.A., 1994, Phys.Rev.B **50**, 5868.
Itie, J. P., Polian,A. Jauberthiecarillon,C. Dartyge,E. Fontaine,A. Tolentino,A. and Tourillon, G. 1989, Phys. Rev. B. **40**, 9709.
Itie, J. P., San Miguel,A. Polian,A. and J. Jap, 1993, Appl. Phys. Part 1, **32**, 711.
Jamieson, J. C., 1963, Science 139, 762.
Jayaraman, A., 1983, Rev. Mod. Phys. **55**, 65
Joannopolous, J. D., and Cohen,M.L., 1976 Solid State Physics **31**
Jones,H. *the theory of Brillouin zones and electronic states in Crystals* (North Holland, Amsterdam, 1962)
Jones, R. O., and Gunnarsson,O. Rev. Mod. Phys. 1989, **61**, 689.
Karki,BB, Ackland,GJ and Crain,J, 1997, J.Phys.CM **9** 8579
Kasper J.S., and Richards S.M., 1964 Acta Crystallogr. **17** 752.
Kelsey,A Ackland,GJ and Clark,SJ 1998 Phys.Rev.B **57**, R2029.
Kelsey,A. 1997 PhD thesis, University of Edinburgh.
Kelsey,A. and Ackland,GJ 2000 J.Phys.CM **12** 32 (2000).
Kim,K. Lambrecht, W.R.L, Segall,B. 1996 Phys Rev B **53**, 16310.
Klotz,S, Besson,JM, Schwoererbohning,M, Nelmes,RJ, Braden,M, Pintschovius,L Appl. Phys. Letters, 1995, **66**, 1557
Klotz S., Besson JM., Braden M., Karch K., Pavone P., Strauch D., and Marshall WG., Phys. Rev. Letters 1997, **79**, 1313
Knittle,E. Wentzcovitch,R.M., Jeanloz,R and Cohen,M.L. 1989, Nature, **337** 349.
Kocinski P and Zbroszczyk M 1995, Semiconductor Sci. and Tech., **10**, 1452
Kohn,W. and Sham,LJ, 1965, Phys.Rev **140** A1133
Lawaetz A, Phys. Rev. B. 1972 **5** , 4039.
Lewis,SP and Cohen,ML 1994 Solid State Comm **89**, 483
Lewis, S. P., and Cohen,M.L., 1993, Phys. Rev. B. **48**, 16144.
Liu,A.Y., Garcia,A., Cohen,M.L. Godwal,B.K. and Jeanloz,R. 1991 Phys. Rev. B. **43**, 1795.
Mao,HK and Bell,PM Science, 1979 **203** 1004.
Marks,NA, McKenzie,DR, Pailthorpe,BA, Bernasconi,M, Parrinello,M Phys Rev B, 1996, **54**, 9703
Marks,NA, McKenzie,DR, Pailthorpe,BA, Bernasconi,M, Parrinello,M Phys.Rev.Lett, 1996, **76**, 768
McGreevy,RL, Howe,MA Ann. Rev Materials Science, 1992, **22**, 217
McMahon M. I., R. J. Nelmes, N. G. Wright, D. R. Allan, 1994, Phys. Rev. B. **50**, 739.
McMahon,MI, Nelmes,RJ, Allan,DR, Belmonte,SA, Bovornratanaraks,T Phys.Rev.Lett, 1998, **80**, 5564
McMahon,MI, Nelmes,RJ Phys.Rev.Lett, 1997, **78**, 3697
McMahon, M. I. and Nelmes,R.J. 1993, Phys. Rev. B. **47**, 8337.
McMahon,MI, Nelmes,RJ Phys.Stat.Solidi B, 1996, **198**, 389
McMahon, M. I., Nelmes, R. J, Wright, N. G., and Allan,D.R. 1993, Phys. Rev. B. **48**, 16246.
McMahon, M. I., Nelmes, R. J., Wright, N. G., and Allan,D.R. 1994, Phys. Rev. B. **50**, 13047.
Mann AB, van Heerden D, Pethica JB and Weihs TP. 2000 J Mater.Res. **15** 1754
Meisalo V., and Kalliomaki M., 1973 High Temp. High Press. **5** 663.
Menoni, CS and Spain, IL 1987, Phys.Rev. B **35** 7520.
Mezouar,M, Besson,JM, Syfosse,G, Itie,JP, Hausermann,D, and Hanfland,M Phys Stat Solidi B, 1996, **198**, 403
Mignot, J.M., Chouteau,G. and Martinez,G 1986, Phys.Rev.B **34** 3150.
Minomura, S and Drickamer, H.G. 1962, J.Phys.Chem.Solids **23**, 451.
Mizushima, K., Yip,S. and Kaxiras,E. 1994, Phys. Rev. B. **50**, 14952.
Mujica, A. and Needs,R.J., 1993, Phys. Rev. B. **48**, 17010.
Mujica, A. and Needs,R.J. 1996, J. Phys. C. **8**, 15 L237.
Mujica, A., Needs,RJ, and Munoz,A. 1995, Phys. Rev. B. **52**, 8881.
Mujica,A, RodriguezHernandez,P, Radescu,S, Needs,RJ and Munoz,A Phys.Stat.Solidi B, 1999, **211**, 39
Mujica,A, Needs,RJ, and Munoz,A Phys.Stat.Solidi B, 1996, **198**, No.1, 461

Mujica,A, Munoz,A, Radescu,S, and Needs,RJ Phys.Stat.Solidi B, 1999, **211**, 345.
Mujica,A, Radescu,S, Munoz,A. and Needs,RJ Phys.Stat.Solidi B, 2001, **223** 379.
Mujica,A, Munoz,A, and Needs,RJ Phys.Rev.B, 1998, **57**, 1344
Mujica, A., and R. J. Needs, 1997 Phys Rev B, **55**,9659; **56**,12653 (Correction)
Mujica,A and Needs,RJ J.Phys.CM 1996, **8**, L237
Needs,RJ and Mujica,A Phys.Rev.B, 1995, **51**, 9652
Munoz, A., and Kunc,K. 1993, Phys. Rev. B. **44**, 10372.
Murnaghan F.D. 1944, Proc. Natl. Acad. Sci. USA **3**, 244.
Nardelli, M. B., Baroni,S. and Gianozzi,P. 1995, Phys. Rev. B. **51**, 8060.
Needs R. J., and Martin,R.M. 1984, Phys. Rev. B. **30**, 5390.
Needs, R. J., and Mujica,A. 1995, Phys. Rev. B. **51**, 9652.
Nelmes,RJ, Liu,H, Belmonte,SA, Loveday,JS, McMahon,MI, Allan,DR, Hausermann,D, and Hanfland,M, Phys.Rev.B, 1996, **53**, R2907.
Nelmes,RJ, McMahon,MI Phys.Rev.Lett, 1996, **77**, 663
McMahon,MI, Nelmes,RJ, Wright,NG, Allan,DR Phys.Rev.B, 1994, **50**, 13047
McMahon,MI, Nelmes,RJ, Wright,NG, Allan,DR Phys.Rev.B, 1994, **50**, 739
Nelmes,RJ, McMahon,MI, Hatton,PD, Crain,J, Piltz,RO Phys.Rev.B, 1993, **48**, 9949
McMahon,MI and Nelmes,RJ Phys.Rev.B, 1993, **47**,8337
Nelmes,RJ, McMahon,MI, Hatton,PD, Crain,J, Piltz,RO Phys Rev B 1993, **47**, 35.
Nelmes,RJ, McMahon,MI, Wright,NG, Allan,DR, Liu,H and Loveday,JS J.Phys.Chem.Solids, 1995, **56**, 539
McMahon,MI, Nelmes,RJ J.Phys Chem Solids, 1995, **56** 485.
Nelmes, R. J., and McMahon,M.I., 1995, Phys. Rev. Lett. **74**, 106 1995, Phys. Rev. Lett. **74**, 2618.
Nelmes, R. J., and McMahon,M.I., 1998, Semiconductors and semimetals, **54** 145.
Nelmes,RJ, McMahon,MI, Belmonte,SA Phys Rev Letters, 1997, **79**, 3668
Nelmes, R. J., and McMahon,M.I., 1996, Phys. Rev. Lett. **77**, 663.
Nelmes, R. J. and McMahon,M.I., J. Synchrotron, 1994, Radiation , **1** , Pt1, 69.
Nelmes, R. J., McMahon,M.I.,, Wright,N.G. and Allan,D.R. 1994, Phys. Rev. Lett. **73**, 1805.
Nelmes, R. J., McMahon,M.I., Wright,N.G. Allan,D.R 1995, Phys. Rev. B. **51**, 15723.
Nelmes, R. J., McMahon,M.I., Wright,N.G. Allan,D.R, Liu,H. Loveday,J.S. 1995, J. Phys. Chem. Solids 56, 539.
Nelmes, R. J., McMahon,M.I., Wright,N.G. Allan,D.R, Loveday,J.S. 1993, Phys. Rev. B. **48**, 9883.
Ohsumi, K., Sueno,S. Nakai,I. Imafuku,M. Morikawa,H. Kimata, M. Nomura,M., Olega, D., Cardona,M. and Muller,H. 1980, Phys. Rev. B **22**, 894.
Olego D., Cardona M., and Vogl P., 1982, Phys. Rev. B **25** 3878.
Olijnyk H., 1992, Phys. Rev. Lett. **68**, 2232.
Olijnyk, H. and Holzapfel,W.B. 1984 J. de Physique, **45**, 153.
Olijnyk,H., Sikka,S.K., Holzapfel.W.B. Phys Letters A, 1984, **103a**, 137.
Pandey,R, Causa,M, Harrison, NM and Seel, M. 1996 J. Phys. CM **8** 3993.
Pandey, R, Jaffe,JE, and Harrison, NM 1994 J. Phys. Chem. Sol **55** 1357.
Parrinello,M. and Rahman,A. 1981 J. Appl. Phys. **52**, 7182.
Parsons,B.J. 1977, Proc.Roy.Soc. A **352**, 397.
Pavone,P, Karch,K, Schutt,O, Windl,W, Strauch,D, Giannozzi,P, Baroni,S Phys.Rev.B, 1993, **48**,3156
Pavone,P. Baroni,S, deGironcoli,S Phys. Rev B,, 1998, **57**, 10421.
Payne, M. C., Teter,M.P., Allan,D.C. Arias,T.A. and Joannopoulos,J.D. 1992, Rev. Mod. Phys. **64**, 1045.
Perdew,JP and Zunger,A, 1981 Phys.Rev.B **23**, 5048
Perdew,JP and Wang,Y 1992 Phys.Rev.B **45**, 13244
Perdew,JP, Burke,K and Ernzerhof,M Phys.Rev.Letts, 1996, **77**, 3865.
Perdew,J.P and Zunger,A. Phys.Rev.B **23**, 5048 (1981).
Perdew, J.P., Chevary,J.A., Vosko,S.H., Jackson, K.A., Pederson,M.R., Singh,D.J. and Fiolhais,C. Phys. Rev. B 46, 6671 (1992)
Perlin, P., C. Jauberthiecarillon, J. P. Itie, A. S. Miguel, I. Gregory, A. Polian, 1992, Phys. Rev. B. **45**, 83.
Perlin, P., Gorczyca,I, Gregory,I. Suski,N. Christensen,N.E. and Polian,A. 1993, Japn. J. Appl. Phys. Suppl. **32**, 334.
Perlin,P, Suski,T, Ager,JW, Conti,G, Polian,A, Christensen,NE, Gorczyca,I, Grzegory,I, Weber,ER, Haller,EE Phys Rev B, 1999, **60** 1480
Pfrommer,BG, Cote,M, Louie,SG, Cohen,ML Phys. Rev B, 1997, **56**, 6662
Olego D., and Cardona M., 1982 Phys. Rev. B **25**, 1151.
Phillips, J. C., and Van Vechtin,J.A., 1970, Phys. Rev. B **2** , 2147.
Piermarini G.J., and Block S., 1975 Rev. Sci. Instrum. **46**, 973.
Piermarini G.J., Block S., Barnett,J.D. and Forman,R.A. 1975 J.Appl.Phys, **46** 2774.
Piltz, R. O., Maclean,JR Clark,SJ Ackland,GJ, Hatton,PD and Crain J., 1995, Phys. Rev B **52**, 4072.
Prins, A. D., Spain,IL Dunstan,DJ 1989, Semicond. Sci. Technol. **4** , 237.
Ribeiro,FJF and Cohen,ML 2000 Phys.Rev.B **62** 11388.

Rodriguez-Hernandez,P., Munoz,A. and Mujica,A 1996 Phys.Stat.Sol (b) **198** 455.
Ruoff, A. L., 1988, Accounts of Chemical Research 21, 223.
Ruoff, A. L., and Li,T. 1995 Annual Rev. Mat. Science 25, 249.
SanMiguel, A., Wright,NG, McMahon,MI and Nelmes,RJ 1995, Phys. Rev. B. **51**, 8731.
Shimomura O, Takamura,K. Fujihisa,H. Fuji,Y. Ohishii,Y. Kikegawa,T. Amemiya,Y. and Matsuhita,T. 1992, Rev. Sci. Instrum. **63**, Pt2B.
Sosin, T. P., Perlin,P. Trzeciakowski,W. and Tober,R. 1995, J. Phys. Chem. Solids **56**, 419.
Spain, I. L., 1987, Contemporary Physics **28**,523.
Spain, I. L., and D.J. Dunstan, 1989, J. Phys. E **22**, 923.
Swift,D. 1999, PhD thesis, University of Edinburgh.
Takemura,K., Schwarz,U., Syassen,K., Christensen, N.E., Hanfland,M. and Novikov,D.L. 2001 Phys.Stat.Solidi B **223**, 385.
Talwar,DN, Thaler,G, Zaranek,S, Peterson,K, Linger,S, Walker,D and Holliday,K 1997, Phys.Rev.B, **55**, 1129
Talwar, D. N., and Vandeveyver,M. 1990, Phys. Rev. B. **41**, 12129.
Tang, M. J., and Yip,S. 1995 Phys. Rev. Lett. **75**, 2738.
Taylor, MB, Barrera, GD, Allan, NL and Barron, THK, 1997 Phys.Rev.B **56** 14380.
Teter,D.M., Hemley,RJ, Kresse,G. and Hafner,J. 1998, Phys.Rev.Letters **80**, 2145
Tersoff,J 1988, Phys.Rev.B **38**, 9902
Thomson,K.T. Wentzcovitch,RM, Bukowinski,MST Science, 1996, **274**, 1880.
Trommer R., Muller, H., Cardona M., and Vogl P., 1980, Phys. Rev. B **21**, 4879.
Tsuji, K., Katayama, Y. Yamamoto,Y., Kanda,H. and Nosaka,H. 1995, J. Phys. Chem. Solids **56**, 559.
Ueno, M., Onodera,A. Shimomura,O. and Takemura,K. 1992, Phys. Rev. B. **45**, 10123.
Ueno, M., Yoshida,M. Onodera,A. Shimomura,O. and Takemura,K. 1992, 1994, Phys. Rev.B.**49**, 14
Vancamp, P. E, Vandoren,V.E. Devreese,J.T. 1992, Solid State Commun. **81**, 23.
Vancamp, P. E, and Vandoren,V.E. 1989, Solid State Commun. **71**, 1055.
Vancamp, P. E, Vandoren,V.E. and Devreese,J.T. 1991, Phys. Rev. B. **44**, 9056.
Vancamp, P. E, Vandoren,V.E. and Devreese,J.T. Int. J of Quantum Chemistry, 1995, **55**, 339.
Vancamp,P.E. and Vandoren,V.E. Solid State Comm., 1995, **95** 173.
Van Camp PE and Van Doren VE 1993 High Pressure Science and Tech. AIP Conf.Proc **309** 171
Venkateswaran, U.D., Chandrasekar,M. Chandrasekar,HR Vojak,BA Chambers,FA and Meese,JM 1986, Phys. Rev. B **33**, 8416.
Venkateswaran, U.D., Cui,CL, Weinstein,BA and Chambers, FA 1992 Phys. Rev. B **45**, 9237.
Vijaykumar, V and Sikka,S.K. 1990, High Pressure Research **4** 306.
Vohra,YK, Weir, ST and Ruoff,AL 1985, Phys. Rev. B. **31**, 7344.
Vohra, Y. K, Brister,KE Desgreniers,S. Ruoff,AL Chang,KJ and Cohen,ML, 1986, Phys. Rev. Lett. **56**, 1944.
Vohra,YK, Xia,H and Ruoff, AL, 1990, Appl.Phys.Lett **57** 2666.
Vohra,YK, Duclos,SJ, Brister,KE and Ruoff,AL Phys.Rev.Lett., 1988, **61**, 574
Vollstadt, H., Ito,E. Akaishi,M. Akimoto.S. and Fukunaga,O. 1990, Proc. Jpn. Acad. B66 7.
Wang J., Yip S., Phillpot S.R., and Wolf D., 1993, Phys. Rev. Lett., **71**, 1993.
Wang, T, Moll,N Cho,K. and Joannopoulos,J, 1999, Phys.Rev.Letters **82** 3304.
Warren,MC and Ackland,GJ, Phys. Chem. Minerals 23, 107-118 (1996).
Warren,MC PhD thesis, University of Edinburgh.
Weinstein B.A., and Piermarini G.J., 1975 Phys. Rev. B **12**, 1172.
Weinstein B.A., Hark, S.K., Burnham,R.D. and Martin, R.M. 1987 Phys.Rev.Lett. **58** 781.
Weinstein B.A., 1977, Solid State Commun. **24**, 595.
Weinstein,B.A. and Zallen,R. Topics in Applied Physics, 1984, **54**, 462
Weir, S. T, Vohra,YK Vanderborgh,CA and Ruoff,AL 1989, Phys. Rev. B. **39**, 1280.
Weir, S. T, Vohra,YK and Ruoff,AL 1987, Phys. Rev. B. **36**, 4543.
Wentzcovitch,RM, Chang,KJ and Cohen,ML 1986 Phys Rev B **34**, 1071
Wentzcovitch,RM, Cohen,ML and Lam,PK Phys.Rev.B, 1987, **36**, 6058
Whitaker,M.F., Webb,S.J., and Dunstan,D.J. 1998 J.Phys.CM, **10** 8611.
Wu,BR and Xu,J Phys.Rev.B, 1999, **60**, 2964
Xia, H., Xia,Q. and Ruoff,A.L. 1993, Phys. Rev. B **47**, 12925.
Xia, Q.,Xia, H., and Ruoff, A.L. 1994, Mod. Phys. Lett.B **8**, 345
Xia, Q., Xia,H. and Ruoff,A.L. 1993, J. Appl. Phys. **73**, 8198.
Yin, M. T., and Cohen,M.L., 1982, Phys. Rev. B 1982, **26**, 3259.
Yin, M. T., and Cohen,M.L., 1982, Phys. Rev. B. **26**, 5668.
Yin, M. T., and Cohen,M.L., 1982, Phys. Rev. B. **26**, 7403.
Yu S. C., Spain,I.L. and Skelton,E.F. 1978, Solid State Commun. **25**, 49.
Yu, P. Y., and Welber,B. 1978, Sol. St. Commun. **25**, 209.
Zhang, S. B. and Cohen,M.L., 1989, Phys. Rev. B. **39**, 1450.
Zunger,A, Kim,K and Ozolins,V, (2001) Phys.Stat.Solidi(b) **223** 369.